cartridges instead of two Sep-Pak C18 cartridges, the extraction efficiencies improved to 27.2±2.8%. To avoid the dead volume of a larger cartridge (500 mg or larger), we employed multiple Oasis HLB Plus cartridges of the smaller size (225 mg) to increase recovery of the intermediate. When three Oasis HLB Plus cartridges were used, one at position 11 and two at position 13, the extraction efficiencies improved to 43.1±2.2%. Using four, five or six Oasis HLB Plus cartridges all improved the efficiency to greater than 50%. As a consequence, we decided to use four Oasis HLB Plus cartridges, one at position 11 and three at position 13, as shown in Fig. 2.

Following the purification, the hydrolysis of ethyl [^{18}F]fluoroacetate was carried out on the cartridges. For [^{18}F]FDG synthesis, this hydrolysis is accomplished at room temperature. Although the hydrolysis of ethyl [^{18}F]fluoroacetate was reported to be performed at 60°C in 3 ml of 1 M aqueous potassium hydroxide solution in a previous paper [9], we anticipated that the hydrolysis of ethyl [^{18}F]fluoroacetate on the cartridges also might proceed at room temperature. Therefore, we examined the hydrolysis of ethyl [^{18}F]fluoroacetate on the cartridges at two temperatures, 60°C and room temperature, and obtained the kinetic curves of hydrolysis (data not shown). In the presence of 1.0 M sodium hydroxide, ethyl [^{18}F]fluoroacetate was completely hydrolyzed in 3.5 min at 60°C and 5.5 min at room temperature. Because longer than 5.5 min was never required, the hydrolysis of ethyl [^{18}F]fluoroacetate was performed at room temperature for 5.5 min.

Because more HLB Plus cartridges were being used, the amount of aqueous sodium hydroxide was increased to 2.7 ml based on experimental results. The concentration of aqueous sodium hydroxide solution, 1.0 M [19], was used without further investigation. About 3.0 ml of 1.0 M aqueous hydrochloric acid solution was required to neutralize the base. The pH of the final solution was adjusted to 5.0–8.0 with 5 ml of 0.2 M aqueous sodium bicarbonate solution, instead of the citrate buffer solution used in the [^{18}F]FDG synthesis.

3.4. Influence of initially added radioactivity

In the present work, different amounts of fluorine-18 radioactivity, from 740 MBq to 14.8 GBq, were used in the radiosynthesis. Radiochemical yields (decay corrected) were calculated to be 49.7±6.0%, 50.9±6.1%, 49.5±5.6% and 50.3±3.7%, in the cases of 740 MBq, 33.7 GBq, 7.4 GBq and 14.8 GBq, respectively (n=3). The data indicate that the radiochemical yield of the final product, sodium [^{18}F]fluoroacetate, did not depend on the initial amount of fluorine-18 radioactivity.

3.5. Analyses of sodium [^{18}F]fluoroacetate

The final solution was analyzed by TLC and HPLC. No fluorine-18 anion was detected in the final solution, and the radiochemical purity of sodium [^{18}F]fluoroacetate was confirmed to be more than 99%. The total radiochemical yield was 50.2±4.8% (n=10, decay corrected). The chemical purity was also assessed by HPLC, and no specific peaks were found except for that of sodium bicarbonate. The pH of the final solution was 7.5±0.2. The total synthesis time was about 32 min. The final solution was also analyzed with GC to show that it contained less than 10 ppm acetonitrile. The pyrogenicity check was carried out using an LAL kit and showed satisfactory results. The absence of Kryptofix 2.2.2 was confirmed with a previously reported method [20]. All the results from the preparation of sodium [^{18}F]fluoroacetate using the TRACERlab MX$_{FDG}$ presented here showed dramatic improvement compared to previous works [9–12].

4. Conclusion

The automated synthesis of sodium [^{18}F]fluoroacetate has been successfully accomplished. Using the commercial [^{18}F]FDG synthesizer TRACERlab MX$_{FDG}$, the final solution can be obtained in 32 min after EOB with a radiochemical yield of 50.2±4.8% (decay corrected). This work widens the application of the TRACERlab MX$_{FDG}$ and should provide users of the TRACERlab MX$_{FDG}$ with easy access to sodium [^{18}F]fluoroacetate for PET imaging.

Acknowledgments

We are grateful to Mr. S. Nakakoji and Mr. K. Hanawa who produced [^{18}F]fluoride for this work, and Mr. S. Kasamatsu for the expert technical assistance. This work was supported by The 21st Century Centers of Excellence Program by Japan Society for the Promotion Science (JSPS), "Biomedical Imaging Technology Integration Program (BITIP)," and by the Research and Development Project Aimed at Economic Revitalization (Leading Project) by the Ministry of Education, Culture, Sports, Technology and Science (MEXT), Japan.

References

[1] Eason CT, Wickstrom M, Turck P, Wright GRG. A review of recent regulatory and environmental toxicology studies on 1080. NZ J Ecol 1999;23(2):129–37.
[2] Guidelines for the safe use of sodium fluoroacetate (1080). New Zealand: Department of Labor; 2002.
[3] Liebecq C, Peters RA. The toxicity of fluoroacetate and the tricarboxylic acid cycle. Biochem Biophys Acta 1949;3:215–30.
[4] Clarke DD. Fluoroacetate and fluorocitrate: mechanism of action. Neurochem Res 1991;16(9):1055–8.
[5] Lear JL, Ackermann RF. Evaluation of radiolabeled acetate and fluoroacetate as potential tracers of cerebral oxidative metabolism. Metab Brain Dis 1990;5(1):45–56.
[6] Ponde DE, Oyama N, Dence CS, Welch MJ. [^{18}F]fluoroacetate, an analog of C-11 acetate for tumor imaging. J Nucl Med 2003; 44:1062P.
[7] Oyama N, Ponde DE, Dence CS, Yokoyama O, Siegel BA, Welch MJ. In vitro and in vivo assessment of F-18 fluoroacetate; a potential analog for tumor imaging. J Nucl Med 2004;45:331P.

[8] Matthies A, Ezziddin S, Ulrich EM, Palmedo H, Biersack HJ, Bender H, et al. Imaging of prostate cancer metastases with ^{18}F-fluoroacetate using PET/CT. Eur J Nucl Med Mol Imaging 2004;31(5):797.

[9] Jeong JM, Lee DS, Chung JK, Lee MC, Koh CS, Kang SS. Synthesis of no-carrier-added [^{18}F]fluoroacetate. J Label Compd Radiopharm 1997;39:395–9.

[10] Sykes TR, Ruth TJ, Adam MJ. Synthesis and murine tissue uptake of sodium [^{18}F]fluoroacetate. Int J Radiat Appl Instrum B 1986;13(5): 497–500.

[11] Tewson TJ, Welch MJ. Preparation and preliminary biodistribution of NCA fluorine-18 fluoroethanol. J Nucl Med 1980;20:559–64.

[12] Bosch AL, Degrado TR, Gatley SJ. Preparation of no carrier added fluorine-18 labeled 16-fluorohexadecanoic and fluoroacetic acids from highly reactive tetraethylammonium [^{18}F]fluoride. Int J Radiat Appl Instrum A 1986;37(4):305–8.

[13] Fuchtner F, Steinbach J, Mading P, Johannsen B. Basic hydrolysis of 2-[^{18}F]Fluoro-1,3,4,6- tetra-*O*-acetyl-D-glucose in the preparation of 2-[^{18}F]Fluoro-2-deoxy-D-glucose. Appl Radiat Isot 1996;47:61–6.

[14] From the website of GE Healthcare. http://www.gehealthcare.com/usen/fun_img/radiopharmacy/products/tracerlabmx.html.

[15] Havbrandt O, Wachtmeister CA. Synthesis of mesyloxyacetic acid and some derivatives. Acta Chem Scand 1968;22:2043–4.

[16] Tasic L, Abraham RJ, Rittner R. Substituent effects on ^{1}H and ^{13}C NMR chemical shifts in α-monosubstituted ethyl acetates: principal component analysis and ^{1}H chemical shift calculations. Magn Reson Chem 2002;40:449–54.

[17] Ponde DE, Dence CS, Schuster DP, Welch MJ. Rapid and reproducible radiosynthesis of [^{18}F]FHBG. Nucl Med Biol 2004;31: 133–8.

[18] Lemaire C, Damhaut P, Lauricella B, Mosdzianowski C, Morelle J-L, Monclus M, et al. Fast [^{18}F]FDG synthesis by alkaline hydrolysis on a low polarity solid phase support. J Label Compd Radiopharm 2002; 45:435–47.

[19] Mosdzianowski C, Lemaire C, Simoens F, Aerts J, Morelle J-L, Luxen A. Epimerization study on [^{18}F]FDG produced by an alkaline hydrolysis on solid support under stringent conditions. Appl Radiat Isot 2002;56:871–5.

[20] Mock BH, Winkle W, Vavrek MT. A color spot test for the detection of Kryptofix 2.2.2 in [^{18}F]FDG preparations. Nucl Med Biol 1997;24: 193–5.

資料(9)

資料 9

Available online at www.sciencedirect.com

ScienceDirect

Nuclear Medicine and Biology 33 (2006) 751–764

NUCLEAR MEDICINE — AND — BIOLOGY

www.elsevier.com/locate/nucmedbio

Alkyl-fluorinated thymidine derivatives for imaging cell proliferation I. The in vitro evaluation of some alkyl-fluorinated thymidine derivatives

Jun Toyohara[a,*], Akio Hayashi[b], Akie Gogami[b], Masahiro Hamada[c], Yoshio Hamashima[c], Takahiro Katoh[c], Manabu Node[c], Yasuhisa Fujibayashi[d]

[a]*Probe Research Section, Department of Molecular Probe, Molecular Imaging Center, National Institute of Radiological Sciences, Chiba 263-8555, Japan*
[b]*Research and Development Division, Research Center, Nihon Medi-Physics Co., Ltd., Chiba 299-0266, Japan*
[c]*Department of Pharmaceutical Manufacturing Chemistry, Kyoto Pharmaceutical University, Kyoto 607-8412, Japan*
[d]*Biomedical Imaging Research Center, University of Fukui, Fukui 910-1193, Japan*

Received 16 January 2006; received in revised form 16 June 2006; accepted 19 June 2006

Abstract

Derivatives of 2′ -deoxyuridine that contain fluoroalkyl groups at the C5 position and derivatives of thymidine that contain fluoroalkyl groups at the N3 position were synthesized and examined in three in vitro assays designed to evaluate their potential as radiopharmaceuticals for imaging cellular proliferation. Three of the former nucleosides and five of the latter were synthesized. The three assays were as follows: (a) phosphoryl transfer assay, which showed that all three of the former nucleosides and four of the latter ones were phosphorylated by recombinant human thymidine kinase 1 (TK1) and that N^3-(2-fluoroethyl)-thymidine (NFT202) was the most potent substrate of the eight nucleosides studied; (b) transport assay, which indicated that all eight nucleosides had good affinity for an 6-[(4-nitrobenzyl)thio]-9-β-D-ribofuranosylpurine-sensitive mouse erythrocyte nucleoside transporter, with inhibition constants in the range of 0.02–0.55 mM; and (c) degradation assay, which showed that all but one of the former nucleosides and none of the latter were degraded by recombinant *Escherichia coli* thymidine phosphorylase (an enzyme that catalyzes the glycosidic bond of thymidine and 2′ -deoxyuridine derivatives). From these in vitro screening assays, we selected NFT202 as a candidate for subsequent in vivo evaluation because this compound met the three minimum requirements of the in vitro screening assays and had the most potent phosphorylation activity as a substrate for recombinant human TK1.

Keywords: Nucleosides; Thymidine kinase; Thymidine phosphorylase; Nucleoside transporter

1. Introduction

The application of current nuclear imaging techniques, such as glucose metabolism, depends basically on the nonspecific phenotype of the tumor. This phenotype dependence is troublesome in several patient management situations [1–4]. Based on recent progress in tumor biology, cancer is best described as a mass of cells with highly elevated and uncontrolled proliferative potential, caused by mutations in cellular growth control genes that are partly inherited and partly generated by spontaneous as well as environmental DNA damage [5]. For that reason and because of the direct link of phenotype to genotype, we have focused on tumor-specific highly elevated cell proliferation.

DNA synthesis for cell proliferation is essential, and thymidine can be rapidly incorporated into newly synthesized DNA via a specific salvage pathway. Based on these findings, many attempts have been made to visualize tumor cell proliferation by using thymidine and 2′-deoxyuridine derivatives [6–13]. However, the rapid degradation of these tracers in vivo results in numerous labeled metabolites, which hampers the measurement of proliferation rates and compromises image quality. The recognition that an electronegative substituent at the 2′-position (α or β configuration) can stabilize thymidine analogs towards enzymatic cleavage of the nucleoside glycosidic bond led to the study of 1-(2-deoxy-2-[^{18}F]fluoro-β-D-arabinofuranosyl)-thymine ([^{18}F]FMAU) for proliferation imaging, given that [^{14}C]FMAU was known to label DNA [14–19]. The first human imaging study with [^{18}F]FMAU illustrated that it was possible to image DNA synthesis in vivo in human tumors [18]. However, an unexpectedly low uptake

* Corresponding author. Tel.: +81 43 206 4041; fax: +81 43 206 3261.
E-mail address: toyohara@nirs.go.jp (J. Toyohara).

0969-8051/$ – see front matter © 2006 Elsevier Inc. All rights reserved.
doi:10.1016/j.nucmedbio.2006.06.003

was seen for proliferative bone marrow in contrast to thymidine and 3′-[^{18}F]fluoro-3′-deoxythymidine ([^{18}F]FLT) [20]. Therefore, this unsolved mechanism of uptake and retention in tumors relative to bone marrow should be explored. From a substrate specificity point of view, these 2′-β-nucleosides, such as 1-(2-deoxy-2-fluoro-β-D-arabinofuranosyl)-thymine (FMAU) and 1-(2-deoxy-2-fluoro-β-D-arabinofuranosyl)-5-iodouracil, are efficient substrates for thymidine kinase 2 (TK2; the mitochondrial isozyme of thymidine kinase) but show only minimal activity with thymidine kinase 1 (TK1; the key enzyme of mammalian DNA synthesis) [21,22]. In a previous report, we found no correlation between the cell proliferation (demonstrated by [^{3}H]thymidine uptake and S-phase fraction) of malignant tumor cells and the uptake of the TK2 selective substrate [^{3}H]arabinothymidine [23]. We therefore concluded that radiopharmaceuticals with a high affinity for TK2 are not suitable agents for the diagnostic imaging of proliferating tissues, despite the fact that 30% of [^{3}H]arabinothymidine was incorporated into DNA.

In 1998, a biologically stable radiofluorine-labeled thymidine analog, [^{18}F]FLT, was developed as a candidate for cell proliferation imaging [20,24,25]. FLT is phosphorylated by TK1, a cell-cycle-regulated isozyme, and it is metabolically retained as 5′-phosphate. This is because FLT lacks a 3′-hydroxyl structure necessary for the polymerase reactions of oligonucleotide synthesis and because FLT 5′-triphosphate can only terminate newly synthesized DNA strands. These characteristics of FLT trapping will induce a discrepancy between FLT uptake and the DNA synthesis phenomenon [26].

Our group has reported on another strategy. Noting the report of Rahim et al. [27] on 5-iodo-4′-thio-2′-deoxyuridine (ITdU), we conducted an experimental study on ^{125}I-labeled ITdU [28,29]. It was preclinically confirmed that ITdU, in which the 4′-oxo of 5-iodo-2′-deoxyuridine had been replaced by 4′-sulfur, is resistant to metabolic decomposition by thymidine phosphorylase (TP) and is an agent that directly reflects DNA synthesis. The results of that study suggested that this tactic could be used to produce a new 4′-thio derivative to supplement the research on the 2′-arabino-F and 3′-F derivative previously developed. As mentioned, in spite of these studies on nucleoside-based imaging agents, there is still a need for a thymidine analog that might prove simpler to use for imaging DNA synthesis and stimulates a more widespread use of such agents. That is why we further tested several thymidine derivatives and introduced a new approach to drug design.

In this paper, we describe studies with thymidine derivatives that contain fluoroalkyl groups at the N3 position and 2′ -deoxyuridine derivatives that contain fluoroalkyl groups at the C5 position. The structures of these derivatives and R designations are shown in Fig. 1 and in the tables, respectively. The chemical structures of 5-(2-fluoroethyl)-2′-deoxyuridine (**1b**; FT202), 5-(fluoromethyl)-4′-thio-2′-deoxyuridine (**1c**; FTS101), 5-(2-fluoroethyl)-4′-thio-2′-deoxyuridine (**1d**; FTS202), N^3-(fluoromethyl)-thymidine (**1e**; NFT201) and N^3-(2-fluoroethyl)-thymidine (**1f**; NFT202) are already known and have been used as antiviral agents, but the corresponding ^{18}F-labeled compounds are not known and have not been used as imaging agents [27,30–33]. We have compared the in vitro phosphorylation rates of these nucleosides with those of recombinant human TK1 by phosphoryl transfer assay. Nucleoside transport inhibition constants (K_i) were measured to evaluate their interaction with the nucleoside transporter. Their stability toward the phosphorolytic enzyme, TP, has been used as an indicator of their metabolic stability. From these in vitro screening assays, we selected NFT202 (**1f**) as a candidate for subsequent in vivo evaluation because this compound surmounted the three minimum requirements of in vitro screening assays and also had the most potent phosphorylation activity as a substrate for recombinant human TK1. In addition, this compound might be amenable to labeling with ^{18}F by the use of a known method.

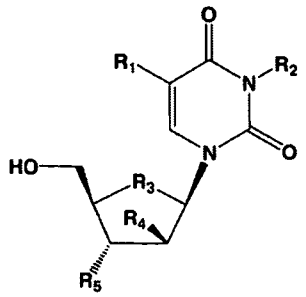

Fig. 1. Structures of evaluated nucleosides. R designations are described in the tables.

However, our companion work describes an in vitro and an in vivo evaluation of NFT202 (**1f**) and reveals that NFT202 was less effective than 3′-deoxy-3′-fluorothymidine (**1j**; FLT). We discuss the pitfalls of our limited selection criteria in our companion paper.

2. Materials and methods

2.1. Chemicals

Thymidine (**1a**), FLT (**1j**) and 5-fluoro-2′ -deoxyuridine (**1k**; FdUrd) were purchased from Sigma-Aldrich Japan KK (Tokyo, Japan). Other reagents for synthesis were purchased from Sigma-Aldrich Japan KK, Wako Pure Chemical Industries, Ltd. (Osaka, Japan), and Tokyo Kasei Kogyo, Co., Ltd. (Tokyo, Japan).

2.2. Synthesis

A summary of the various syntheses is given below. Experimental details and the characterization of compounds are described in succeeding sections.

All isolated materials were shown to be pure by nuclear magnetic resonance (NMR; free of obvious impurities) and by thin-layer chromatography (TLC; homogeneous material).

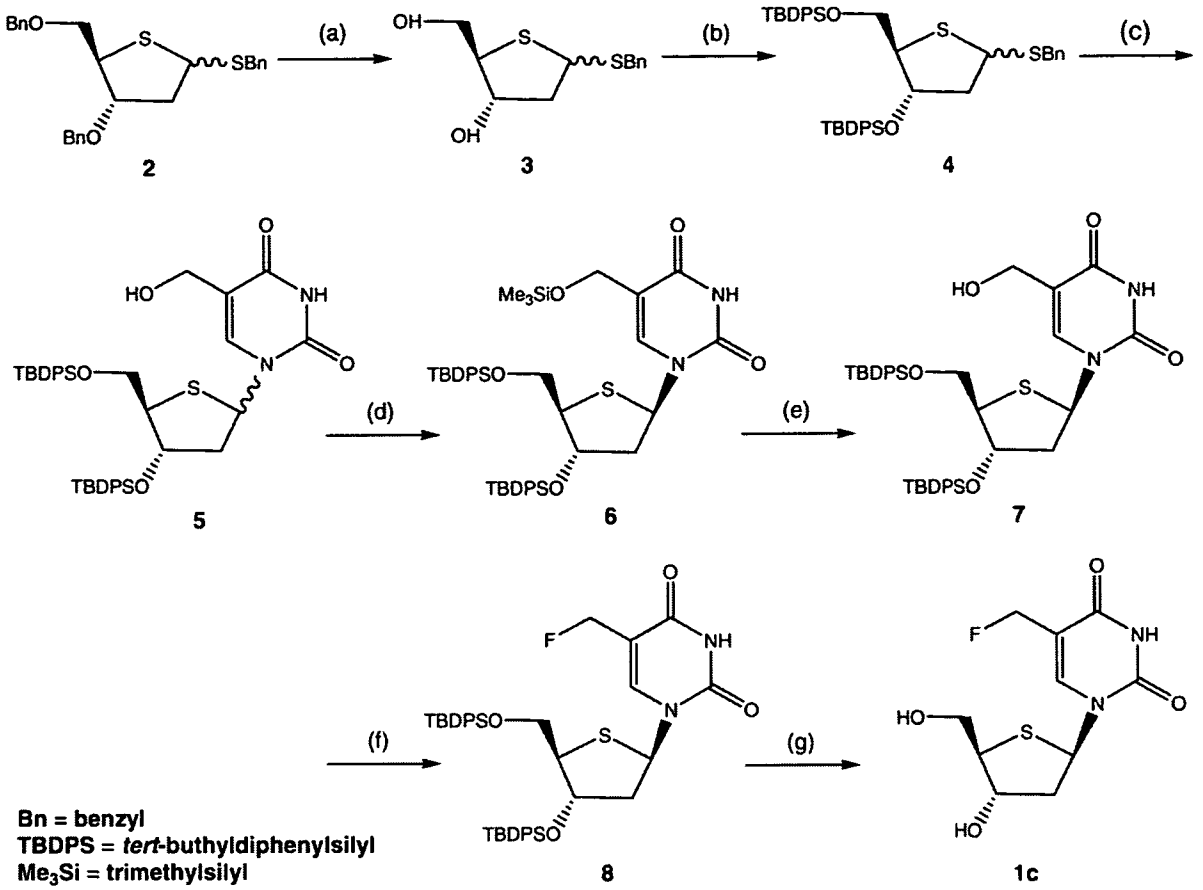

Fig. 2. Synthesis of FTS101. Conditions: (a) BCl_3, CH_2Cl_2, −78°C. (b) TBDPSCl, imidazole, DMF, 0°C. (c) (i) 5-Hydroxymethyluracil, BTMSA, MS4Å, DMF, 0°C; (ii) NIS, RT. (d) TMSCl, TEA, CH_3CN, 0°C. (e) 6 N HCl, $CHCl_3/CH_3CN$, 0°C. (f) DAST, CH_2Cl_2, −20°C. (g) TBAF, THF, RT.

Compound **1b** was synthesized by a previously described method [30]. The synthetic procedures of Compounds **1c** and **1d** differed from that of 5-fluoro-4′-thio-2′-deoxyuridine (**1l**). The coupling reaction of benzyl 3,5-di-*O*-benzyl-2-deoxy-1,4-dithio-D-*erythro*-pentofuranoside (**2**) with a silylated base in the presence of *N*-iodosuccinimide (NIS) and molecular sieves was processed successfully [34]. However, subsequent debenzylation by Lewis acid hardly proceeded, and the desired compounds (**1c** and **1d**) were not obtained. As shown in Figs. 2 and 3, Compounds **1c** and **1d** were obtained by replacing the protecting groups of Compound **2** with di-*O*-*tert*-butyldiphenylsilyl. Moreover, separation of the α/β mixture of Compound **1c** was conducted by trimethylsilylation of the hydroxylmethyl residue of 3′,5′-di-*O*-*tert*-butyldiphenylsilyl-5-hydroxymethyl-4′-thio-2′-deoxy-β-uridine (**7**). Compound **1e** was synthesized by a previously described method [32]. The N^3 alkyl-fluorination of thymidine derivatives [**1f**, N^3-(3-fluoropropyl)-thymidine (**1g**), N^3-(2-fluoroethyl)-4′-thio-2′-deoxyuridine (**1h**) and 1-(2-deoxy-2-fluoro-β-D-arabinofuranosyl)-N^3-(2-fluoroethyl)-thymine (**1i**)] was conducted in a one-step reaction from the corresponding nucleoside (β anomer) by adapting

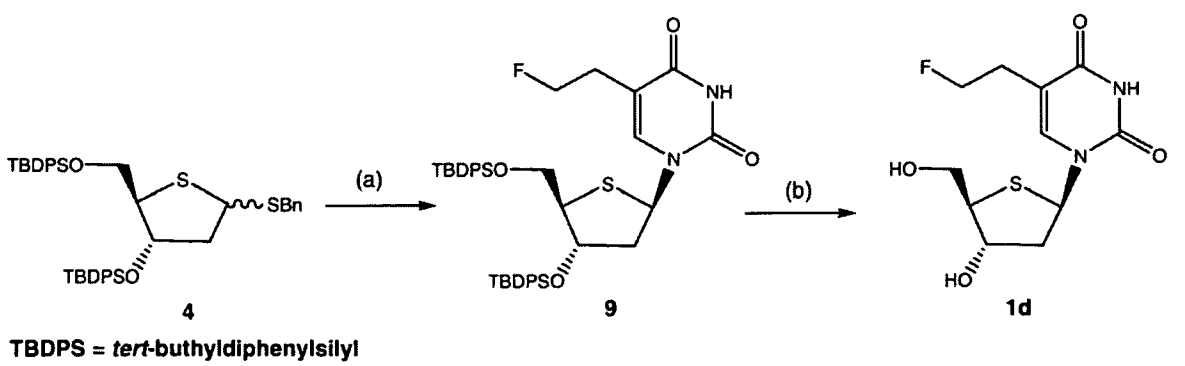

Fig. 3. Synthesis of Compound **1d** (FTS202). Conditions: (a) (i) 5-(2-Fluoroethyl)uracil, BTMSA, CH_3CN, RT; (ii) MS4Å, NIS, DMF, RT. (b) TBAF, THF, RT.

previously described procedures [35,36]. Fluoroalkyl-tosylate or fluoroalkyl-bromide was added to a solution containing a weak base and a nucleoside in either a *N*,*N*-dimethylformamide (DMF)/acetone mixture, DMF, or tetrahydrofuran (THF) at a mild reaction temperature [from room temperature (RT) to 80°C], yielding the target compounds at high yields (72–100%). While alkylations at other positions on the nucleoside are possible, selective alkylation on the N3 position of pyrimidine was reported [35,37,38].

*2.3. 5-(2-Fluoroethyl)-2′-deoxyuridine (**1b**; FT202)*

5-(2-Acetylhydroxyethyl)uracil was synthesized using γ-butyrolactone as a starting material, according to the method of Fissekis et al. [39]. Furthermore, FT202 was prepared from 5-(2-acetylhydroxyethyl)uracil according to the method of Griengl et al. [30]. The pure β anomer of 3′,5′-di-*O*-*p*-toluoyl-5-(2-fluoroethyl)-2′-deoxyuridine was crystallized in ethanol at 4°C, as reported in the literature [30]. After deprotection, the resultant compound (**1b**) was obtained. The melting point of Compound **1b** was in agreement with the previously reported temperature [30]. Its purity was assessed by a conspicuous absence of impurities in the ^{1}H NMR spectrum and in high-performance liquid chromatography (HPLC; purity, 96.9%):

^{1}H NMR (CD_3OD, 500 MHz) δ 7.92 (s, 1H), 6.26 (t, J=6.5 Hz, 1H), 4.53 (dtd, J=47.0, 5.5 and 3.0 Hz, 2H), 4.37 (quint, J=3.0 Hz, 1H), 3.92 (q, J=3.0 Hz, 1H), 3.90 (dd, J=12.0 and 3.0 Hz, 1H), 3.73 (dd, J=12.0 and 3.5 Hz, 1H), 2.71 (td, J=5.5 and 2.0 Hz, 1H), 2.68 (td, J=5.5 and 1.5 Hz, 1H), 2.26 (m, 1H), 2.21 (m, 1H)
UV λ_{max} (CH_3OH)=266 nm
m_p=153°C
fast atom bombardment mass spectroscopy (FABMS), m/z=297 [M+Na].

The conditions of HPLC analysis are described in Section 2.15.

*2.4. 5-(Fluoromethyl)-4′-thio-2′-deoxyuridine (**1c**; FTS101)*

The schematic diagram for the synthesis of FTS101 is depicted in Fig. 2. Compound **2** was prepared with a seven-step synthesis starting from 2-deoxy-D-*erythro*-pentose, following the procedure of Dyson et al. [40]. To a dichloromethane solution (25 ml) of Compound **2** (3.85 g, 8.8 mmol) was added borontrichloride (1.0 M in dichloromethane, 40 ml, 40 mmol) at −78°C. The resultant mixture was stirred at −78°C for 4 h. The mixture was added to a methanol–aqueous solution of ammonia (1:1 vol/vol, 40 ml), then the organic layer was separated. The aqueous layer was rinsed with chloroform. The combined organic layer was dried with sodium sulfate, filtered and then concentrated in vacuo. The crude material was purified by silica gel column chromatography (eluent, acetone:hexane=1:1) to give benzyl-2-deoxy-1,4-dithio-D-*erythro*-pentofuranoside (**3**) (1.5 g, 66%).

To a DMF (30 ml) solution of Compound **3** (1.5 g, 5.85 mmol) was added *tert*-butyldiphenylsilylchloride (TBDPSCl; 3.8 ml, 11.7 mmol) and imidazole (1.79 g, 23.4 mmol) at 0°C. The resultant mixture was stirred overnight at RT. The mixture was concentrated in vacuo to remove DMF. The residue was extracted with ethyl acetate. The organic layer was washed with water, dried with sodium sulfate, filtered and then concentrated in vacuo. The crude material was purified with silica gel column chromatography (eluent, hexane:ethyl acetate=10:1) to give benzyl-3,5-di-*O*-*tert*-butyldiphenylsilyl-2-deoxy-1,4-dithio-D-*erythro*-pentofuranoside (**4**) (3.88 g, 90%).

To a DMF (28 ml) suspension of 5-hydroxymethyluracil (737 mg, 5.18 mmol) were added bis(trimethylsilyl)acetylene (BTMSA; 2.56 ml, 11.3 mmol), Compound **4** (3.8 g, 5.18 mmol) and molecular sieves 4 Å (MS4Å; ca. 460 mg) at 0°C, and the mixture was stirred for 30 min. The mixture was then added to a DMF (10 ml) solution of NIS (1.23 g, 5.18 mmol) and stirred at RT overnight. The mixture was concentrated in vacuo to remove DMF. The residue was added to ice water, and an aqueous solution of 5% sodium thiosulfate then was extracted with ethyl acetate. The organic layer was washed with 5% aqueous solution of sodium thiosulfate, 5% aqueous solution of sodium hydrogen carbonate and a saturated aqueous solution of sodium chloride. It was then dried with sodium sulfate, filtered and concentrated in vacuo. The crude material was purified by silica gel column chromatography (eluent, hexane:ethyl acetate=1:1) to give a mixture of Compound **5** (1.2 g, 31%).

To an acetonitrile (40 ml) solution of Compound **5** (2.69 g, 3.58 mmol) were added triethylamine (TEA; 3 ml, 21.5 mmol) and trimethylsilylchloride (TMSCl; 1.36 ml, 10.7 mmol) at 0°C. After stirring for 5 min, the mixture was concentrated in vacuo. The residue was extracted with ethyl acetate. The organic layer was washed with a diluted aqueous solution of sodium hydrogen carbonate and a saturated aqueous solution of sodium chloride, dried with sodium sulfate, filtered and concentrated in vacuo. The crude material was purified by silica gel column chromatography (eluent, hexane:ethyl acetate=2:1) to give 3′,5′-di-*O*-*tert*-butyldiphenylsilyl-5-trimethylsilyloxymethyl-4′-thio-2′-deoxyuridine (**6**) (1.15 g, 39%) and its anomer (1.4 g, 47%):

Compound **6**
^{1}H NMR ($CDCl_3$, 400 MHz) δ 8.52 (br.s, 1H), 7.63–7.27 (m, 21H), 6.56 (dd, J=8.8 and 6.2 Hz, 1H), 4.48 (dd, J=3.0 and 2.0 Hz, 1H), 4.30 (s, 2H), 3.68–3.63 (m, 2H), 3.49 (dd , J=12.4 and 10.4 Hz, 1H), 2.14–2.07 (m, 1H), 1.44–1.38 (m, 1H), 1.07 (s, 9H), 0.94 (s, 9H), 0.01 (s, 9H).

To a chloroform (10 ml)–acetonitrile (20 ml) solution of Compound **6** (1.15 g, 1.39 mmol) was added 6 N hydrochloric acid (0.6 ml) at 0°C. The mixture was stirred for 10 min, neutralized with 5% aqueous solution of sodium hydrogen carbonate and concentrated in vacuo to remove the organic solvent. The residue was extracted with ethyl

acetate. The organic layer was washed with water, dried with sodium sulfate, filtered and concentrated in vacuo. The crude material was purified by silica gel column chromatography (eluent, hexane:ethyl acetate=1:1) to give 3′,5′-di-*O*-*tert*-butyldiphenylsilyl-5-hydroxymethyl-4′-thio-2′-deoxy-β-uridine (**7**; 1.01 g, 97%):

^{1}H NMR ($CDCl_3$, 200 MHz) δ 7.54 (br.s, 1H), 7.64–7.26 (m, 21H), 6.53 (dd, J=8.1 and 6.3 Hz, 1H), 4.43 (br.s, 1H), 4.11 (d, J=2.4 Hz, 1H), 2.28–2.21 (m, 1H), 1.75–1.60 (m, 1H), 1.07 (s, 9H), 0.96 (s, 9H).

To a dichloromethane (12 ml) solution of Compound **7** (1.0 g, 1.33 mmol) was added a dichloromethane (12 ml) solution of (dimethylamino)sulfur trifluoride (DAST; 264 μl, 2.0 mmol) at −20°C, followed by stirring for 20 min. The mixture was poured onto crushed ice then extracted with chloroform. The organic layer was dried with sodium sulfate, filtered and concentrated in vacuo. The crude material was purified by silica gel column chromatography (eluent, hexane:ethyl acetate=2:1) to give 3′,5′-di-*O*-*tert*-butyldiphenylsilyl-5-fluoromethyl-4′-thio-2′-deoxyuridine (**8**) (740 mg, 74%).

To a THF (6.5 ml) solution of Compound **8** (1.03 g, 1.36 mmol) was added tetrabutylammonium fluoride (TBAF; 1.0 M in THF, 4.1 ml, 4.1 mmol), followed by stirring at RT for 35 min. The mixture was purified by silica gel column chromatography (prepacked by dichloromethane eluent, THF:dichloromethane=2:1) to give Compound **1c** (FTS101, 300 mg, 80%). The purity of Compound **1c** was assessed by the conspicuous absence of impurities in the ^{1}H NMR spectrum and in HPLC (retention time, 13.6 min; purity, 98.7%). HPLC was performed with a C18 (5-μm) analytical column [150×4.6 (i.d.) mm, Mightysil RP-18 GP Aqua; Kanto Chemical, Tokyo, Japan]. Elution was conducted by CH_3OH:H_2O:trifluoroacetic acid (TFA)=10:90:0.1 at a flow rate of 0.8 ml/min and was monitored at 254 nm:

^{1}H NMR [dimethyl sulfoxide (DMSO)-d_6, 400 MHz] δ 11.58 (s, 1H), 8.33 (d, J=4.0 Hz, 1H), 6.25 (t, J=7.2 Hz, 1H), 5.27 (d, J=4.0 Hz, 1H), 5.19 (t, J=5.6 Hz, 1H), 5.08 (d, J=88 Hz, 2H), 4.37 (m, 1H), 3.59 (m, 1H), 3.58 (m, 1H), 3.29 (m, 1H), 2.20 (dd, J=7.2 and 4.0 Hz, 2H)
UV λ_{max} (CH_3OH)=267 nm
FABMS, m/z=299 [M+Na].

*2.5. 5-(2-Fluoroethyl)-4′-thio-2′-deoxyuridine (**1d**; FTS202)*

The schematic diagram for the synthesis of FTS202 is depicted in Fig. 3. 5-(2-Acetylhydroxyethyl)uracil was synthesized, using γ-butyrolactone as a starting material, according to the method of Fissekis et al. [39]. Furthermore, 5-(2-fluoroethyl)uracil was prepared from 5-(2-acetylhydroxyethyl)uracil, according to the method of Griengl et al. [30]. To an acetonitrile (2.5 ml) suspension of 5-(2-fluoroethyl)uracil (237 mg, 1.50 mmol) was added BTMSA (630 mg, 3.10 mmol), and the resultant mixture was stirred at RT for 1 h. The reaction mixture was added to MS4Å (ca. 1.0 g), a DMF (2.5 ml) solution of Compound **4** (733 mg, 1.0 mmol) and NIS (270 mg, 1.20 mmol). The resultant mixture was stirred at RT for 24 h and filtered, and the filtrate was extracted with diethyl ether. The combined organic layer was washed with a 5% aqueous solution of sodium thiosulfate and a saturated aqueous solution of sodium hydrogen carbonate and brine. It was then dried with sodium sulfate, filtered and concentrated in vacuo. The crude material was purified by silica gel column chromatography (eluent, hexane:ethyl acetate=3:7→2:3→1:1) and silica gel recycle HPLC to give 3′,5′-di-*O*-*tert*-butyldiphenylsilyl-5-(2-fluoroethyl)-4′-thio-2′-deoxyuridine (**9**) (180 mg, 24%) and its anomer (227 mg, 30%):

Compound **9**
^{1}H NMR ($CDCl_3$, 400 MHz) δ 8.67 (s, 1H), 7.67–7.29 (m, 21H), 6.54 (dd, J=8.6 and 6.2 Hz, 1H), 4.49–4.42 (m, 2H), 4.38–4.31 (m, 1H), 3.62–3.03 (m, 3H), 2.49 (t, J=5.9 Hz, 1H), 2.42 (t, J=5.5 Hz, 1H), 2.22 (ddd, J=13.2, 6.2 and 3.5 Hz, 1H), 1.68–1.61 (m, 1H), 1.04 (s, 9H), 0.96 (s, 9H)
^{13}C NMR (100 MHz, $CDCl_3$) δ 162.7, 150.2, 138.2, 135.7, 135.7, 135.6, 135.4, 133.1, 133.1, 133.0, 132.6, 130.0, 130.0, 129.9, 127.9, 127.8, 127.8, 110.4, 82.1, 80.4, 77.2, 76.0, 65.9, 61.0, 58.8, 42.5, 28.3, 28.1, 26.9, 26.8, 19.2, 19.1
FABMS, m/z=789 [M+Na]
High-resolution mass spectroscopy (HRMS) for $C_{43}H_{51}FN_2O_4SSi_2Na$: calculated=789.2220, found=789.2994.

Anomer
^{1}H NMR ($CDCl_3$, 400 MHz) δ 9.01 (s, 1H), 8.14 (s, 1H), 7.60–7.28 (m, 20H), 6.22 (dd, J=8.1 and 3.1 Hz, 1H), 4.56 (t, J=6.1 Hz, 1H), 4.46–4.42 (m, 2H), 3.76 (td, J=6.0 and 2.4 Hz, 1H), 3.38 (dd, J=10.6 and 6.5 Hz, 1H), 3.26 (dd, J=10.6 and 6.5 Hz, 1H), 2.72–2.38 (m, 3H), 2.19 (dt, J=14.3 and 2.8 Hz, 1H), 1.07 (s, 9H), 0.96 (s, 3H)
^{13}C NMR (100 MHz, $CDCl_3$) δ 163.1, 150.7, 140.5, 135.7, 135.7, 135.6, 135.5, 132.8, 132.8, 132.7, 130.2, 130.1, 129.8, 127.9, 127.9, 127.7, 109.7, 109.6, 82.3, 80.7, 77.6, 77.2, 65.7, 62.5, 60.5, 44.6, 28.6, 28.4, 27.0, 26.7, 19.1.

To a THF (17.5 ml) solution of Compound **9** (1.34 g, 1.75 mmol) was added TBAF (1.0 M in THF, 6.99 ml, 6.99 mmol) at 0°C, and the resultant mixture was stirred at RT. After 2 h, the reaction mixture was concentrated in vacuo. The crude material was purified by silica gel column chromatography (eluent, chloroform:methanol=9:1) and was recrystallized from methanol to give FTS202 (403 mg, 79%). The purity of Compound **1d** was assessed by the conspicuous absence of impurities in the ^{1}H NMR spectrum and in HPLC (purity, 99.7%):

^{1}H NMR (DMSO-d_6, 400 MHz) δ 11.4 (s, 1H), 7.91 (s, 1H), 6.27 (t, J=7.4 Hz, 1H), 5.26 (d, J=3.8 Hz, 1H),

5.18 (t, J=5.4 Hz, 1H), 4.50 (dt, J=40.0 and 6.4 Hz, 2H), 4.37 (quint, J=3.5 Hz, 1H), 3.60 (m, 2H), 3.29 (m, 1H), 2.68 (td, J=6.2 and 3.3 Hz, 1H), 2.62 (td, J=6.0 and 3.7 Hz, 1H), 2.18 (d, J=4.0 Hz, 1H), 2.16 (d, J=3.8 Hz, 1H)
^{13}C NMR (DMSO-d_6, 75 MHz) δ 163.0, 150.6, 138.8, 109.1 (d, J=6.2 Hz), 82.8, 80.6, 73.4, 63.5, 60.2, 59.0, 41.2, 27.7 (d, J=21.2 Hz)
^{13}C NMR (100 MHz, $CDCl_3$) δ 163.0, 150.6, 138.8, 109.1 (d, J=6.2 Hz), 82.8, 80.6, 73.4, 63.5, 60.2, 59.0, 41.2, 27.7 (J=21.2 Hz)
UV λ_{max} (CH_3OH)=270 nm
m_p=196°C
FABMS, m/z=291 [M+H]
HRMS for $C_{11}H_{16}FN_2O_4S$: calculated=291.0815, found=291.0821.

The conditions of HPLC analysis are described in Section 2.15.

2.6. N^3-(fluoromethyl)-thymidine (**1e**; NFT201)

NFT201 was synthesized, using thymidine as a starting material, according to the procedure of Ogilvie et al. [32]. The purity of Compound **1e** was assessed by the conspicuous absence of impurities in the ^{1}H NMR spectrum and in HPLC (purity, 89.2%). The structure of the compound was based on its constitution (mass spectrometry), and the similarity of its ^{1}H NMR spectrum was based on other closely related molecules (thymidine and NFT202):

^{1}H NMR (CD_3OD, 500 MHz) δ 7.89 (s, 1H), 6.28 (t, J=6.5 Hz, 1H), 5.97 (d, J=50.5 Hz, 2H), 4.40 (quint, J=3.0 Hz, 1H), 3.92 (q, J=3.0 Hz, 1H), 3.80 (dd, J=12.5 and 3.0 Hz, 1H), 3.73 (dd, J=12.5 and 3.5 Hz, 1H), 2.28 (ddd, J=13.5, 6.5 and 3.5 Hz, 1H), 2.28 (ddd, J=13.5, 6.5 and 3.5 Hz, 1H), 2.22 (dd, J=13.5 and 3.5 Hz, 1H), 1.91 (s, 3H)
UV λ_{max} (CH_3OH)=271 nm
m_p=67–70°C
FABMS, m/z=275 [M+H]
HRMS for $C_{11}H_{16}FN_2O_5$: calculated=275.1044, found=275.0984.

The conditions of HPLC analysis are described in Section 2.15.

2.7. N^3-(2-fluoroethyl)-thymidine (**1f**; NFT202)

Using 2-fluoroethanol as a starting material, 2-fluoroethyltosylate was synthesized according to the method of Edgell and Parts [41]. 2-Fluoroethyltosylate (3.6 g, 17 mmol), potassium carbonate (4.6 g, 33 mmol) and thymidine (2.0 g, 8.3 mmol) were dissolved in an acetone:DMF (1:1) mixed solvent (500 ml), and the mixture was heated at 50°C for 7 h under argon atmosphere. The solvent was removed by rotary evaporation, and the desired product (**1f**; NFT202, 2.2 g, 94%) was purified by silica gel column chromatography (chloroform:methanol=5:1). The purity of Compound **1f** was assessed by the conspicuous absence of impurities in the ^{1}H NMR spectrum and in HPLC (purity, 98.4%):

^{1}H NMR (CD_3OD, 500 MHz) δ 7.85 (s, 1H, H-5), 6.29 (t, H-1′, $J_{1',2'a}$=$J_{1',2'b}$=5.6 Hz), 4.62, 4.53 (each t, each 1H, H-2″), 4.39 (m, 1H, H-3′), 4.25 (m, 2H, H-1″), 3.91(dd, 1H, H-5′ a, $J_{5'a,4'}$=2.4, $J_{5'a,5'b}$=9.6 Hz), 3.80 (dd, 1H, H-5′ b, $J_{5'b,4'}$=2.8, $J_{5'b,5'a}$=9.6 Hz), 3.72 (m, 1H, H-4′), 2.27 (ddd, 1H, H-2′ a, $J_{2'a,3'}$=2.8, $J_{2'a,1'}$=6.0, $J_{2'a,2'b}$=10.8 Hz), 2.21 (m, 1H, H-2′ b), 1.89 (s, 3H, 5-CH_3)
UV λ_{max} (CH_3OH)=267 nm
FABMS, m/z=289 [M+H]
HRMS for $C_{12}H_{18}FN_2O_5$: calculated =289.1200, found= 189.1230.

The conditions of HPLC analysis are described in Section 2.15.

2.8. N^3-(3-fluoropropyl)-thymidine (**1g**; NFT203)

1-Bromo-3-fluoropropane (5.0 g, 36 mmol), TBAF (16.2 g, 62 mmol) in THF (62 ml) and thymidine (1.5 g, 6.2 mmol) were dissolved in THF (40 ml), and the mixture was stirred at RT for 1 h under argon atmosphere. The solvent was removed by rotary evaporation, and the desired product (NFT203, 2.0 g, 100%) was purified by silica gel column chromatography (chloroform:methanol=5:1). The purity of Compound **1g** was assessed by the conspicuous absence of impurities in the ^{1}H NMR spectrum and in HPLC (purity, 97.8%):

^{1}H NMR (CD_3OD, 500 MHz) δ 7.82 (s, 1H, H-5), 6.28 (t, H-1′, $J_{1',2'a}$=$J_{1',2'b}$=5.6 Hz), 4.51, 4.42 (each t, each 1H, H-2″), 4.39 (m, 1H, H-3′), 4.04 (m, 2H, H-1″), 3.91 (dd, 1H, H-5′ a, $J_{5'a,4'}$=2.4, $J_{5'a,5'b}$=9.6 Hz), 3.80 (dd, 1H, H-5′ b, $J_{5'b,4'}$=2.8, $J_{5'b,5'a}$=9.6 Hz), 3.72 (m, 1H, H-4′), 2.27 (ddd, 1H, H-2′ a, $J_{2'a,3'}$=2.8, $J_{2'a,1'}$=6.0, $J_{2'a,2'b}$=10.8 Hz), 2.21 (m, 1H, H-2′ b), 1.95 (m, 1H, H-2″), 1.89 (s, 3H, 5-CH_3)
UV λ_{max} (CH_3OH)=268 nm
FABMS, m/z=303 [M+H]
HRMS for $C_{13}H_{20}FN_2O_5$: calculated=303.1356, found= 303.1372.

The conditions of HPLC analysis are described in Section 2.15.

2.9. N^3-(2-fluoroethyl)-4′-thio-2′-deoxyuridine (**1h**; NFTS202)

4′-Thio-thymidine was prepared from Compound **2**, according to the method of Otter et al. [34]. 2-Fluoro-1-bromoethane (127 mg, 1 mmol), cesium carbonate (195 mg, 0.6 mmol) and 4′ -thio-thymidine (129 mg, 0.5 mmol) were dissolved in DMF (5 ml), and the mixture was heated at 80°C for 10 h under argon atmosphere. The solvent was removed by rotary evaporation, and the desired product (NFTS202, 122 mg, 80%) was purified by silica gel column chromatography (chloroform:methanol=20:1). The purity

of Compound **1h** was assessed by the conspicuous absence of impurities in the ^{1}H NMR spectrum and in HPLC (purity, 92.7%):

^{1}H NMR (CD_3OD, 500 MHz) δ 6.60 (dd, H-1′, $J_{1',2'a}$=4.6, $J_{1',2'b}$=7.0 Hz), 5.74 (m, 1H, H-3′), 4.81 (dd, 1H, H-5′ a, $J_{5'a,4'}$ =2.4, $J_{5'a,5'b}$=10.0 Hz), 4.54–4.77 (m, 2H, H-5′ b, H-1″b), 4.60 (m, 1H, H-1″a), 4.55 (m, 1H, H-4′), 4.35 (m, 1H, H-2″a), 4.33 (m, 1H, H-2″a), 2.99 (ddd, 1H, H-2′ a, $J_{2'a,3'}$ =1.2, $J_{2'a,1'}$ =4.6, $J_{2'a,2'b}$=11.2 Hz), 2.83 (m, 1H, 2″-OH), 2.30 (ddd, 1H, H-2′ b, $J_{2'b,3'}$ =5.2, $J_{2'b,1'}$ =7.0, $J_{2'b,2'a}$=11.2 Hz), 1.65 (s, 3H, 5-CH_3)
UV λ_{max} (CH_3OH)=271 nm
FABMS, *m/z*=305 [M+H]
HRMS for $C_{12}H_{18}FN_2O_4S$: calculated=305.0971, found=305.1013.

The conditions of HPLC analysis are described in Section 2.15

*2.10. 1-(2-Deoxy-2-fluoro-β-D-arabinofuranosyl)-N^3-(2-fluoroethyl)-thymine (**1i**; NFAU202)*

FMAU was prepared by a four-step synthesis starting from 1,3,5-tri-*O*-benzoyl-α-D-ribofuranose, according to the procedure of Wilds and Damha [42]. 2-Fluoroethyltosylate (541 mg, 2.5 mmol), potassium carbonate (630 mg, 4.6 mmol) and FMAU (323 mg, 1.2 mmol) were dissolved in acetone:DMF (1:1; 30 ml), and the mixture was heated at 50°C for 8 h under argon atmosphere. The solvent was removed by rotary evaporation, and the desired product (NFAU202, 272 mg, 72%) was purified by silica gel column chromatography (chloroform:methanol=5:1). The purity of Compound **1i** was assessed by the conspicuous absence of impurities in the ^{1}H NMR spectrum and in HPLC (purity, 97.5%):

^{1}H NMR (CD_3OD, 500 MHz) δ 7.73 (s, 1H, H-5), 6.20 (dd, 1H, H-1′, $J_{1',F}$=17 Hz, $J_{1',2'}$ =4.0 Hz), 5.03 (dt, 1H, H-2′, $J_{2',F}$=52 Hz, $J_{1',2'}$ =$J_{2',3'}$ =2.5 Hz), 4.58 (dd, 2H, H-2″, $J_{2'',F}$=47 Hz, $J_{1',2'b}$=5.0 Hz), 4.32 (m, 1H, H-3′), 4.28 (m, 2H, H-1″), 3.91 (m, 1H, H-4′), 3.86 (dd, 1H, H-5′ a, $J_{5'a,4'}$ =12.0, $J_{5'a,5'b}$=4.0 Hz), 3.76 (dd, 1H, H-5′ b, $J_{5'b,4'}$ =12.0, $J_{5'b,5'a}$=4.0 Hz), 2.66 (s, 3H, 5-CH_3)
UV λ_{max} (CH_3OH)=265 nm
FABMS, *m/z*=307 [M+H]
HRMS for $C_{12}H_{17}F_2N_2O_5$: calculated=307.1106, found=307.1072.

The conditions of HPLC analysis are described in Section 2.15.

*2.11. 5-Fluoro-4′-thio-2′-deoxyuridine (**1l**; FTS901)*

The schematic diagram for the synthesis of Compound **1l** (FTS901) is depicted in Fig. 4. To an acetonitrile (8.7 ml) suspension of 5-fluorouracil (1.70 g, 13.0 mmol) was added BTMSA (5.66 g, 27.8 mmol), and the resultant mixture was stirred at RT for 2 h. The reaction mixture was added to MS4Å (ca. 4.3 g), an acetonitrile (8.7 ml) solution of Compound **2** (3.80 g, 8.70 mmol) and NIS (2.35 g, 10.4 mmol). The resultant mixture was stirred at RT for 22 h, filtered and concentrated in vacuo. The residue was dissolved with ethyl acetate, then the organic layer was washed with a 5% aqueous solution of sodium thiosulfate and a saturated aqueous solution of sodium hydrogen carbonate and brine. It was then dried with magnesium sulfate, filtered and concentrated in vacuo. The crude material was purified by silica gel column chromatography (eluent, hexane:ethyl acetate=3:2) to give 3′,5′-di-*O*-benzyl-5-fluoro-4′-thio-2′-deoxyuridine (**10**) (3.49 g, 91%, α:β=2:1):

β anomer ^{1}H NMR ($CDCl_3$, 300 MHz) δ 8.25 (d, *J*=6.6 Hz, 1H), 8.05 (br.s, 1H), 7.37–7.28 (m, 10H), 6.40 (t, *J*=6.6 Hz, 1H), 4.61–4.48 (m, 4H), 4.22 (q, *J*=3.7 Hz, 1H), 3.69 (q, *J*=3.7 Hz, 1H), 3.80–3.60 (m, 2H), 2.51 (ddd, *J*=13.6, 6.6 and 4.0 Hz, 1H), 2.15 (ddd, *J*=13.6, 7.7 and 4.4 Hz, 1H).

To a dichloromethane (3 ml) solution of Compound **10** (β anomer: 221 mg, 0.50 mmol) was added boron trichloride (1.0 M in dichloromethane solution, 2.0 ml, 2.0 mmol) at −78°C, and the resultant mixture was stirred at −78°C for 1 h. The mixture was quenched with a methanol

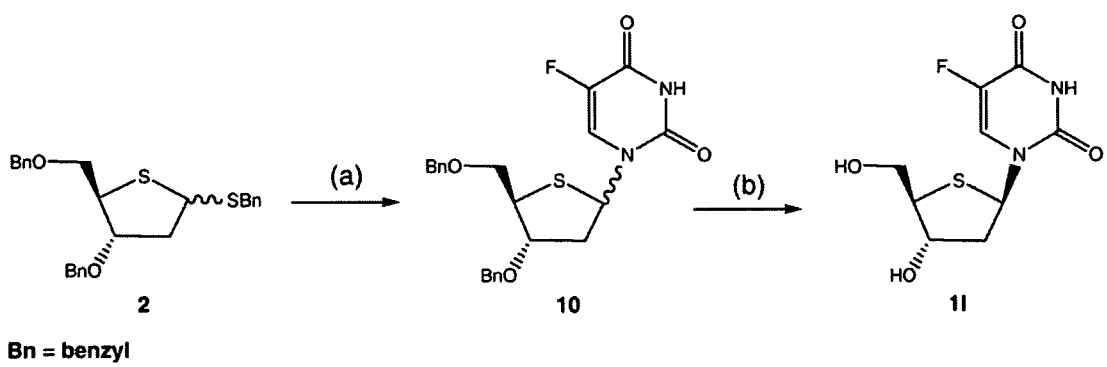

Fig. 4. Synthesis of Compound **1l** (FTS901). Conditions: (a) (i) 5-Fluorouracil, BTMSA, CH_3CN, RT; (ii) MS4Å, NIS, DMF, RT. (b) BCl_3, CH_2Cl_2, −78°C.

solution of ammonia (2.0 M, 3.0 ml), after which the mixture was warmed to RT and concentrated in vacuo. The residue was diluted with methanol and filtered, and the filtrate was concentrated in vacuo. The crude material was purified by silica gel column chromatography (eluent, chloroform:methanol=9:1) to give Compound **11** (FTS901, 59 mg, 45%). The purity of Compound **11** was assessed by the conspicuous absence of impurities in the ^{1}H NMR spectrum and in HPLC (purity, 97.6%):

^{1}H NMR (DMSO-d_6, 300 MHz) δ 11.84 (br.s, 1H), 8.33 (d, J=7.3 Hz, 1H), 6.23 (t, J=7.3 Hz, 1H), 5.24–5.19 (m, 1H), 4.35 (m, 1H), 3.65–3.55 (m, 2H), 3.31–3.28 (m, 1H), 2.25–2.15 (m, 2H)
^{13}C NMR (DMSO-d_6, 75 MHz) δ 157.5, 150.2, 142.1, 126.4, 74.4, 64.0, 61.8, 59.9, 42.2
UV λ_{max} (CH_3OH)=272 nm
FABMS, m/z=263 [M+H]
HRMS for $C_9H_{12}FN_2O_4S$: calculated=263.0502, found=263.0508.

The conditions of HPLC analysis are described in Section 2.15.

2.12. Expression and purification of recombinant human thymidine kinase

The preparation of recombinant human TK1 was carried out as described previously, with minor modifications [35]. The cDNA for human TK1 was amplified by polymerase chain reaction with plasmid pTK11 as template [43] and a pair of primers (5′-sense primer, 5′ CCATATGAGCTGCATTAACCTG; 3′-reverse complement primer, 5′ CGGGATCCCTCAGTTGGCAG) to create an *Nde*I site at the 5′-end and a *Bam*HI site at the 3′-end of the fragment. After treatment with *Nde*I and *Bam*HI, the TK1 fragment was ligated to plasmid pET-14b (EMD Biosciences Inc., San Diego, CA), which had been digested previously with the same restriction enzymes, to yield the expression plasmid pETMS207No.5. After being sequenced to confirm the correct insertion, pETMS207No.5 was transfected into *Escherichia coli* BL21 (DE3) pLys host cells. The expression of recombinant TK1 was induced with 0.4 mM isopropyl β-D-thiogalactopyranoside, and the protein was purified by affinity chromatography on chelated His·Bind resin (EMD Biosciences Inc.). The calculated molecular weight was 28 kDa for recombinant human TK1, and sodium dodecyl sulfate–polyacrylamide gel electrophoresis (SDS-PAGE) showed that the purity of TK1 was >95% (Fig. 5).

2.13. Phosphoryl transfer assay

Phosphoryl transfer assay with recombinant human TK1 was carried out as described previously, with minor modifications [35]. Briefly, nucleosides were dissolved in DMSO to make 100-mM stock solutions. The assays were carried out in reaction mixtures of 100 μM nucleosides (0.25% DMSO), 1 mM [γ-^{33}P]adenosine 5′-trisphosphate

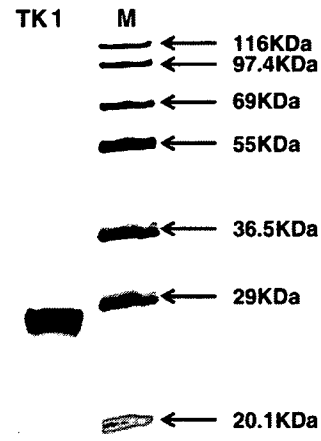

Fig. 5. SDS-PAGE of recombinant TK1 preparations. Two hundred nanograms of purified TK1 was loaded onto 12% gel. M, molecular weight markers.

(Amersham Biosciences, Piscataway, NJ), 50 mM Tris–HCl (pH 7.6), 5 mM $MgCl_2$, 15 mM NaF, 125 mM KCl, 10 mM dithiothreitol and 0.5% bovine serum albumin. The reaction was initiated by the addition of 60 ng of purified recombinant human TK1, and the reaction mixture was incubated for 15 min at 37°C. After being heated to 100°C for 3 min to stop the reaction, the mixture was centrifuged, and 2-μl samples were applied to PEI cellulose TLC plates (Merck Ltd., Darmstadt, Germany). The TLC plates were developed with isobutyric acid:ammonium hydroxide:water (66:1:33) for 12 h. The radioactivity on the plate was measured and quantified by a bioimaging analyzer (BAS-1500; Fuji Photo Film Co., Tokyo, Japan).

2.14. Transport assay

Transport assay was carried out as described previously, with minor modifications [44,45]. Briefly, 9-week-old male ddY mice were purchased from Japan SLC Inc. (Shizuoka, Japan) and were held for 1 week prior to the study. All procedures were performed in accordance with institutional guidelines (Guidelines for Animal Experiments, University of Fukui). The mice were asphyxiated with CO_2; blood was collected into a 3.8% citrate solution by cardiac puncture and used on the same day. After the removal of plasma and buffy coat, packed erythrocytes were washed with buffered saline (140 mM NaCl, 1.4 mM $MgSO_4$ and 18 mM Tris–HCl, at pH 7.4) and suspended in the same medium with a hematocrit of 11%. Nucleoside influx was initiated by the rapid addition of cell suspension to the buffered saline containing [2-^{14}C]thymidine (2.11 GBq/mmol; Amersham Biosciences) at four concentrations (0.05–0.5 mM) alone or together with various concentrations of test nucleosides. After 3 s, transport was terminated by the addition of 6-[(4-nitrobenzyl)thio]-9-β-D-ribofuranosylpurine (NBMPR; Sigma-Aldrich, St. Louis, MO) at a final concentration of 10 μM. Cells were pelleted

by an Eppendorf microcentrifuge (Model 5415D; Eppendorf Co., Ltd., Hamburg, Germany) at 12,800×*g* for 1 min and washed once with NBPMR solution. Cell pellets were extracted and chilled with 5% perchloric acid. After at least 30 min at 4°C, portions of the extracts were removed and counted in ACSII (Amersham Biosciences) by a liquid scintillation counter (LSC-5000; Aloka, Tokyo, Japan). The radioactivity trapped in the extracellular space of the pellet was measured in triplicate as a zero-time value by reversing the order in which NBMPR and nucleoside were added to the cells. This value was subtracted from the radioactivity of influx samples.

2.15. Degradation assay

To evaluate the stability of the N1–C′ 1 glycosidic bond, we tested the degradation of nucleosides by recombinant *E. coli* TP. Degradation assay was carried out as described previously, with minor modifications [46]. Briefly, the reaction mixture (final volume, 0.2 ml) contained 0.1 M potassium phosphate buffer (pH 7.4), 20 nmol of compounds and 0.015 U of recombinant *E. coli* TP (Sigma). The reaction was carried out at 25°C for 5, 15, 30 and 60 min, and terminated by adding 2 N perchloric acid (final concentration, 4%). After neutralization with potassium hydroxide, the resultant precipitate was removed by centrifugation. The supernatant was filtrated through a 4-mm Millex Syringe Filter Unit (Millipore, Bedford, MA), and a 10-μl aliquot was injected into the HPLC with a C18 (5-μm) analytical column [150×4.6 (i.d.) mm, Mightysil RP-18 GP Aqua; Kanto Chemical]. Elution was conducted by CH_3OH:H_2O:TFA [solvent compositions of CH_3OH:H_2O:TFA were as follows: 5:95:0.1 for FdUrd (**1k**); 10:90:0.1 for thymidine (**1a**); 15:85:0.1 for FT202 (**1b**), NFT201 (**1e**) and FTS901 (**1l**); 20:80:0.1 for FTS202 (**1d**), NFT203 (**1g**) and FLT (**1j**); 25:75:0.1 for NFT202 (**1f**) and NFAU202 (**1i**); and 30:70:0.1 for NFTS202 (**1h**)] at a flow rate of 0.8 ml/min and was monitored at 254 nm. Retention times were as follows: thymidine (**1a**), 8.4 min; FT202 (**1b**), 6.8 min; FTS202 (**1d**), 8.6 min; NFT201 (**1e**), 14.8 min; NFT202 (**1f**), 12.3 min; NFT203 (**1g**), 10.5 min; NFTS202 (**1h**), 8.4 min; NFAU202 (**1i**), 11.3 min; FLT (**1j**), 9.5 min; FdUrd (**1k**), 7.4 min; and FTS901 (**1l**), 7.0 min. Each compound was quantified by a comparison with the standard curve using the HPLC peak area of each standard compound.

3. Results

3.1. Phosphoryl transfer assay

The TK1 substrate characteristics of nucleosides were screened in phosphoryl transfer assays as a substrate for the recombinant human TK1 [47,48]. The data are summarized in Table 1. Among alkyl-fluorinated nucleosides, NFT202 (**1f**) had the highest value. The relative order of phosphorylation rates was as follows: thymidine (**1a**)>FdUrd (**1k**)>NFT202 (**1f**)=FLT (**1j**)>FTS101 (**1c**)>NFT201 (**1e**)=NFTS202 (**1h**)=FTS901 (**1l**)>FTS202 (**1d**)=NFT203 (**1g**)=FT202 (**1b**)>NFAU202 (**1i**). No correlation was observed between phosphorylation rates and fluoroalkyl length at the N3 position of thymidine. The 4′-thio substitution of FT202 did not reduce phosphorylation rates. In contrast, 4′ -thio substitution of NFT202 (**1f**) and FdUrd (**1k**) significantly reduced phosphorylation rates; the 2′-β-fluorine substitution of NFT202 (**1f**) further reduced such rates.

3.2. Transport assay

Transport assay was carried out as described previously, with minor modifications [44,45]. The concentration dependence of thymidine influx was portrayed on a Hanes–Woolf plot [49], yielding kinetic parameters of K_m=0.26±0.1 mM and V_{max}=17.54±6.82 pmol/μg packed erythrocytes/s. Competition among nucleosides with thymidine for entry at an external transporter site was demonstrated in influx competition experiments with [2-^{14}C]thymidine. The data were plotted according to Dixon [50]; examples are shown in Fig. 6A. For all compounds tested, the lines intersected at points above the [*I*] axis. Assuming that these data represent competitive inhibition [51], K_i values were determined by

Table 1
Phosphorylation of nucleosides by recombinant TK1, and K_i values of nucleosides in influx competition with thymidine

Compound	R_1	R_2	R_3	R_4	R_5	Phosphorylation (pmol/μg protein/h)	Relative phosphorylation	K_i (mM)
Thymidine (**1a**)	CH_3	H	O	H	OH	3008.05±749.40	1	0.26 (K_m)
FT202 (**1b**)	$F(CH_2)_2$	H	O	H	OH	697.03±87.20	0.23±0.03	0.53
FTS101 (**1c**)	FCH_2	H	S	H	OH	1117.08±87.28	0.37±0.03	0.55
FTS202 (**1d**)	$F(CH_2)_2$	H	S	H	OH	801.64±242.84	0.27±0.08	0.23
NFT201 (**1e**)	CH_3	FCH_2	O	H	OH	987.95±546.99	0.33±0.18	0.38
NFT202 (**1f**)	CH_3	$F(CH_2)_2$	O	H	OH	1424.32±218.82	0.47±0.07	0.53
NFT203 (**1g**)	CH_3	$F(CH_2)_3$	O	H	OH	486.49±198.59	0.26±0.06	0.51
NFTS202 (**1h**)	CH_3	$F(CH_2)_2$	S	H	OH	906.61±168.76	0.30±0.06	0.02
NFAU202 (**1i**)	CH_3	$F(CH_2)_2$	O	F	OH	17.42±0.71	0.01±0.00	0.51
FLT (**1j**)	CH_3	H	O	H	F	1431.89±100.59	0.48±0.03	2.69
FdUrd (**1k**)	F	H	O	H	OH	2571.06±151.38	0.85±0.05	0.70
FTS901 (**1l**)	F	H	S	H	OH	915.87±83.5	0.30±0.03	0.88

The results represent the mean±S.D. of at least three independent experiments.

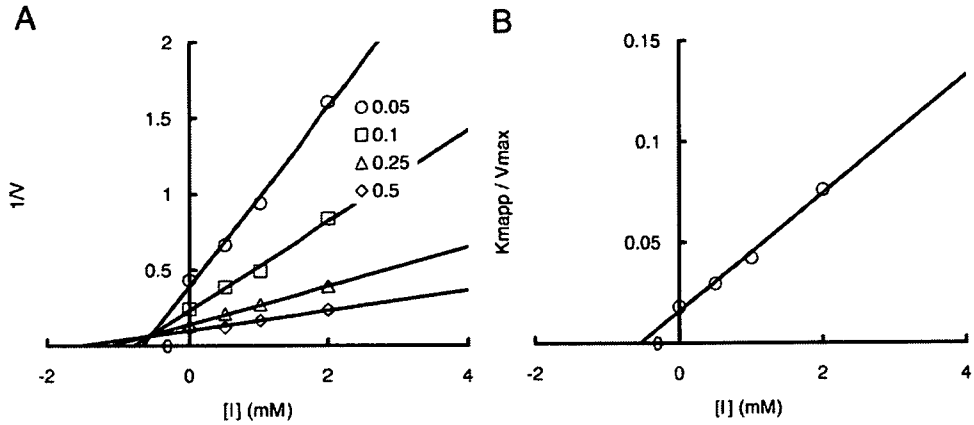

Fig. 6. An example of plots used for determining K_i values for nucleosides in influx competition experiments with thymidine. (A) An example of Dixon plots [50,51] of inhibition data. Each point represents the mean value of duplicate measurements from a single-cell suspension. Ordinates are expressed as picomoles of thymidine per microgram of packed erythrocytes per second, while those of the abscissa are FTS101 (**1c**) concentrations (in millimolars). Thymidine concentrations (mM) are shown in the legend. The lines were fitted by linear regression analysis. (B) K_{mapp} and V_{max} values were determined at each inhibitor concentration according to Eisenthal and Cornish-Bowden [52]. Shown is a replot of the ratios of these values as a function of FTS101 (**1c**) concentration [51]. [Units of the ordinate are expressed as: mM (pmol thymidine/μg packed erythrocytes/s)$^{-1}$.] The lines were fitted by linear regression analysis.

plotting influx competition data according to Eisenthal and Cornish-Bowden [52] to obtain K_{mapp} and V_{max} values and by replotting the ratio of these parameters as a function of [*I*] [51]; examples are shown in Fig. 6B. The K_i values are given in Table 1. These data showed that each of the eight nucleosides had an affinity for the transporter. FTS202 (**1d**) had affinities comparable to those of thymidine. The affinities of NFTS202 (**1h**) were 10 times those of thymidine. The other six alkyl-fluorinated nucleosides showed affinities that were 1.4–2.0 times lower than that of thymidine. FdUrd (**1k**) and FTS901 (**1l**) each showed affinities that were three times lower than that of thymidine. FLT (**1j**) showed affinities that were 10 times lower.

3.3. Degradation assay

Degradation assay was carried out as described previously, with minor modifications [46]. Table 2 shows the results. Except for FT202 (**1b**), there was no detectable glycosidic bond cleavage for 60 min in any of the alkyl-fluorinated nucleosides during incubations with recombinant *E. coli* TP. In contrast, under the same experimental conditions, thymidine (**1a**) underwent rapid glycosidic bond cleavage to give 57%, 89%, 98% and 99% thymidine (**1a**) degradation at 5, 15, 30 and 60 min, respectively. FdUrd (**1k**) and FTS901 (**1l**) also showed significant glycosidic bond cleavage to give 13%, 29%, 46% and 66% FdUrd (**1k**) degradation and 3%, 6%, 10% and 18% FTS901 (**1l**) degradation at 5, 15, 30 and 60 min, respectively. NFT202 (**1b**) underwent only slight time-dependent degradation to give 3%, 4% and 7% NFT202 (**1b**) degradation at 15, 30 and 60 min, respectively. As expected from previous findings, FLT (**1j**) did not show any significant glycosidic bond cleavage during the 60-min incubation with recombinant *E. coli* TP.

Table 2
Nucleosides as substrates for recombinant *E. coli* TP

Compound	R_1	R_2	R_3	R_4	R_5	Remaining nucleosides (%)				
						0 min	5 min	15 min	30 min	60 min
Thymidine (**1a**)	CH_3	H	O	H	OH	100.0±1.1	43.1±0.1	10.6±0.2	2.3±0.1	1.0±0.0
FT202 (**1b**)	$F(CH_2)_2$	H	O	H	OH	100.0±0.2	98.2±0.2	97.4±0.3	95.9±0.3	93.3±0.1
FTS101 (**1c**)	FCH_2	H	S	H	OH	ND	ND	ND	ND	ND
FTS202 (**1d**)	$F(CH_2)_2$	H	S	H	OH	100.0±0.2	99.4±0.3	99.1±0.3	99.3±0.2	98.9±0.1
NFT201 (**1e**)	CH_3	FCH_2	O	H	OH	100.0±2.4	100.9±1.7	98.7±1.7	101.7±0.3	102.0±0.9
NFT202 (**1f**)	CH_3	$F(CH_2)_2$	O	H	OH	100.0±0.5	98.8±1.2	98.7±1.0	99.6±0.9	99.0±0.5
NFT203 (**1g**)	CH_3	$F(CH_2)_3$	O	H	OH	100.0±0.7	99.7±0.6	99.5±0.4	98.0±0.1	99.4±0.2
NFTS202 (**1h**)	CH_3	$F(CH_2)_2$	S	H	OH	100.0±0.6	98.9±0.4	99.0±0.5	98.9±0.4	99.2±0.4
NFAU202 (**1i**)	CH_3	$F(CH_2)_2$	O	F	OH	100.0±0.1	99.4±0.2	99.2±0.4	99.2±0.4	99.1±0.2
FLT (**1j**)	CH_3	H	O	H	F	100.0±1.4	100.1±0.4	98.5±0.7	100.5±0.5	100.4±0.5
FdUrd (**1k**)	F	H	O	H	OH	100.0±0.3	87.1±0.3	71.2±0.4	54.4±0.1	34.1±0.9
FTS901 (**1l**)	F	H	S	H	OH	100.0±0.3	97.5±0.1	94.2±1.0	89.6±0.3	82.2±0.3

Values represent the mean±S.D. of at least three independent experiments of the remaining nucleoside as percentages of the total nucleoside in the reaction (100 μmol/L).
ND, not determined.

4. Discussion

In the last four decades, deoxynucleoside analogs have become increasingly important in the treatment of viral diseases and cancers. Nucleoside analogs are prodrugs requiring 5′-phosphorylation to form active nucleotides that can function as inhibitors of viral or cellular replication processes. Therefore, when labeled with a suitable radionuclide, some of these compounds have potential as radiopharmaceuticals for the noninvasive diagnosis of tumor cell proliferation. To be effective, they should: be selectively phosphorylated by TK1, be amenable to labeling with a positron-emitting or a single-photon-emitting radionuclide, have good in vivo stability and be transported across the cell membrane.

The present study examined those in vitro screens and finally selected NFT202 as a candidate for subsequent in vivo evaluation. This compound may be amenable to labeling with ^{18}F according to known methods.

All bioactive nucleosides have a β-configuration. In this study, Compounds **1b**, **1c**, **1d** and **1l** were obtained as α/β mixtures. The separation of α and β anomers of 3′,5′-di-*O*-*p*-toluoyl-5-(2-fluoroethyl)-2′-deoxyuridine was conducted by crystallization, as previously reported [30]. The melting point of Compound **1b** was also in agreement with the previously reported temperature (β anomer) [30].

The α and β anomers of Compounds **6**, **9** and **10** were easily separated by silica gel column chromatography. Compound **1l** was identified as a β anomer from the references [34]. The melting point of Compound **1d** was in agreement with the previously reported temperature of β anomer [27]. The β-isomer of Compound **1c** was rationally assigned by the result of a comparison of ^{1}H NMR with related β anomers (Compounds **1d** and **1l**).

The rationale of this study's drug design was based on the knowledge of 5-substituted 2′-deoxyuridines and carboranyl thymidine analogs. Many 5-substituted 2′-deoxyuridines, such as 5-fluoro-deoxyuridine, 5-chloro-deoxyuridine, 5-iodo-deoxyuridine, 5-bromo-deoxyuridine and 5-ethyl-2′-deoxyuridine, are good substrates for TK1 [47,48,53–56]. Analogs of 5-substituted 2′-deoxyuridines with bulky substitutions, such as 5-propenyl, 5-(2-chloroethyl)-2′-deoxyuridine and 5-(2-bromovinyl)-2′-deoxyuridine, are poor substrates for TK1 [53–55]. Therefore, we tried to evaluate the derivatives of 2′-deoxyuridine that contained a short-length fluoroalkyl chain at the C5 position, such as 5-(2-fluoroethyl), 5-(fluoromethyl)-4′-thio and 5-(2-fluoroethyl)-4′-thio derivatives of 2′-deoxyuridine. These 5-fluoroalkyl-substituted 2′-deoxyuridine derivatives were phosphorylated by human recombinant TK1. Among them, the compact 5-fluoromethyl substitution was the most effective substrate for TK1. However, the 5-fluoromethyl derivative is thought to be difficult to label with ^{18}F because attempts to synthesize the labeling precursor failed due to the labile nature of the leaving group. Thymidine analogs with methyl, ethyl and isopropyl, as well as various bulky *o*-carboranylalkyl substituents at the N3 position, were found to be surprisingly good substrates for TK1 [35,47,48,55–57]. These data indicate that TK1 can tolerate bulky groups at the N3 position of thymidine. In accordance with this hypothesis, TK1 effectively phosphorylated N^3-(fluoromethyl), N^3-(2-fluoroethyl), N^3-(3-fluoropropyl) and N^3-(2-fluoroethyl)-4′-thio derivatives of thymidine. Very recently, NFT202 was found to inhibit the phosphorylation of thymidine by recombinant TK1 [33]. Consistent with our results, NFT202 in that study retained its affinity for TK1 (IC_{50}=77–81 μg/ml). As expected by the poor phosphorylation activity of the parent fluorinated thymidine analog FMAU [21,22], its derivative (Compound **1i**) showed only minimal activity.

Nucleosides are hydrophilic and diffuse slowly across cell membranes. It is now well established that the permeation of nucleosides across the plasma membrane of mammalian cells is complex and is mediated by multiple transport proteins known as nucleoside transporters [58]. These transporters fall into two basic classes: (a) equilibrative (facilitated diffusion) carriers, which mediate both the influx and efflux of nucleosides, and (b) concentrative Na^+-dependent carriers, which, under physiological conditions, mediate only influx [58–61]. Based on sensitivity to 6-[(4-nitrobenzyl)thio]-9-β-D-ribofuranosylpurine (NBMPR), equilibrative transporters have been classified into two subtypes, equilibrative sensitive (*es*) and equilibrative insensitive (*ei*) [61–65]. The *es* subtype binds NBMPR with high affinity (K_d=1–10 nM) [66]. In contrast, the *ei* subtype is not affected by NBMPR at nanomolar concentrations and becomes inhibited only at high NBMPR concentrations (>10 μM) [66]. These two equilibrative transporters (*es* and *ei*) have been described in a large number of tumor cells and normal tissues. Especially, human tumor cell lines express predominantly NBMPR-sensitive transporters [67]. In contrast, concentrative transporters have been found predominantly in normal tissues, and only a limited number have been found in tumor cells [67]. Therefore, we focused on the transport assay with the NBMPR-sensitive mouse erythrocyte nucleoside transporter. However, inhibition constants, determined from our nucleoside transport assay, are assumed to reflect affinities for external binding sites on the transporter. Therefore, our results do not exactly provide evidence that the nucleoside transporter transports extracellular nucleosides into the cell. Additionally, in in vivo imaging, the expression and functional characteristics of nucleoside transporter families in the absorptive/excretory organs and target/nontarget cells will have important effects on the pharmacokinetics of tracers. Certainly, nucleoside transporters are crucial in determining the intracellular bioavailability and systemic disposition of nucleoside analogs. Knowledge of nucleoside transporters is important in the evaluation and prediction of the kinetics and targeting of nucleoside analogs. In this respect, our restricted transport screening system is

not helpful for predicting biodistribution. Therefore, our screening results cannot be applied directly beyond the in vitro situation.

Surprisingly, without any modification in the sugar moiety, thymidine that contains fluoroalkyl groups at the N3 position [N^3-(fluoromethyl)-thymidine, N^3-(2-fluoroethyl)-thymidine and N^3-(3-fluoropropyl)-thymidine] was not degraded during the 60-min incubations with recombinant *E. coli* TP. In contrast, thymidine was efficiently converted to thymine. Al-Madhoun et al. [47] reported that thymidine analogs containing the *o*-carboranylalkyl group at the 3-position were not substrates of recombinant TP. Our present finding also supports their results.

The development of a molecular imaging probe for positron emission tomography is based on a detailed understanding of cellular and molecular biochemistry. From this point of view, a recent report evaluating the kinetic uptake and retention of FLT in A549 cells should serve as a model for evaluating nucleoside analogs [25]. The DNA salvage pathway involves a futile cycle for nucleoside phosphorylation and dephosphorylation mediated by TK1 and a nucleotidase (dNT). This cycle poses an issue for interpreting tracer uptake values, since it provides a mechanism for the loss of established activity in cells. In proliferating cells, nucleoside analog metabolism takes place within the anabolic arm of the DNA salvage pathway. TK1 controls entry into the salvage pathway and converts intracellular nucleoside analogs to their nucleotide monophosphates [68]. Subsequent phosphorylations by other kinases within the DNA synthesis pathway [thymidylate kinase (TMPK) and nucleotide diphosphate kinase] lead to the added presence of nucleoside diphosphate and nucleoside triphosphate within cells. Intracellular thymidine labels DNA so rapidly that the impact of the retrograde synthesis of thymidine from thymidine triphosphate is negligible. Therefore, as was done for FLT, knowledge of the activities that dNT and TMPK have with regard to new nucleoside analogs would definitively show what analogs are appropriate for further study [25]. In fact, our companion work describes an in vitro and an in vivo evaluation of NFT202 (**1f**) showing that NFT202 (**1f**) was less effective than FLT (**1j**). Consequently, our limited selection criteria were not sufficient for discovering new nucleoside analogs for cell proliferation imaging.

In conclusion, derivatives of 2′-deoxyuridine that contain fluoroalkyl groups at the C5 position and derivatives of thymidine that contain fluoroalkyl groups at the N3 position were synthesized and examined in three in vitro assays designed to evaluate their potential as radiopharmaceuticals for imaging cellular proliferation. From these in vitro screening assays, we selected NFT202 as a candidate for subsequent in vivo evaluation because this compound met the three basic criteria of in vitro screening assays and also had the most potent phosphorylation activity as a substrate for recombinant human TK1. Additionally, this compound can be made amenable to labeling with ^{18}F according to known methods. Further investigation of the feasibility of ^{18}F-labeled NFT202 (**1f**) as a cell proliferation marker is described in separate papers.

Acknowledgments

We thank Mr. Kenji Frutuka for his excellent assistance with mass spectrometry analyses.

References

[1] Kubota R, Yamada S, Kubota K, Ishiwata K, Tamahashi N, Ido T. Intratumoral distribution of fluorine-18-fluorodeoxyglucose in vivo: high accumulation in macrophages and granulation tissues studied by microautoradiography. J Nucl Med 1992;33:1972–80.

[2] Yamada Y, Uchida Y, Tatsumi K, Yamaguchi T, Kimura H, Kitahara H, et al. Fluorine-18-fluorodeoxyglucose and carbon-11-methionine evaluation of lymphadenopathy in sarcoidosis. J Nucl Med 1998;39:1160–6.

[3] Strauss LG. Fluorine-18 deoxyglucose and false-positive results: a major problem in the diagnostics of oncological patients. Eur J Nucl Med 1996;23:1409–15.

[4] Shreve PD, Anzai Y, Whal RL. Pitfalls in oncologic diagnosis with FDG PET imaging: physiologic and benign variants. Radiographics 1999;19:61–77.

[5] Thorgeirsson SS, Okayama H. The United States–Japan cooperative cancer research program seminar on "Cell cycle control and cancer". Jpn J Cancer Res 1998;89:1093–7.

[6] Eary JF, Mankoff DA, Spence AM, Berger MS, Olshen A, Link JM, et al. 2-[C-11]Thymidine imaging of malignant brain tumors. Cancer Res 1999;59:615–21.

[7] Martiat P, Ferrant A, Labar D, Cogneau A, Boc C, Michel JL, et al. In vivo measurement of carbon-11 thymidine uptake in non-Hodgkin's lymphoma using positron emission tomography. J Nucl Med 1998;29:1633–7.

[8] Shields AF, Mankoff DA, Link JM, Graham MM, Eary JF, Kozawa SM, et al. Carbon-11-thymidine and FDG to measure therapy response. J Nucl Med 1998;39:1757–62.

[9] Vander Broght T, Pauwels S, Lambotte L, Labar D, De Maeght S, Stroobandt G, et al. Brain tumor imaging with PET and 2-[carbon-11]thymidine. J Nucl Med 1994;35:974–82.

[10] Van Eijkeren ME, De Schryver A, Goethals P, Poupeye E, Schelstraete K, Lemahieu I, et al. Measurement of short term ^{11}C-thymidine activity in human head and neck tumours using positron emission tomography (PET). Acta Oncol 1992;31:539–43.

[11] Blasberg RG, Roelcke U, Weinreich R, Beattie B, Ammon K, Yonekawa Y, et al. Imaging brain tumor proliferative activity with [^{124}I]iododeoxyuridine. Cancer Res 2000;60:624–35.

[12] Tjuvajev J, Muraki A, Ginos J, Berk J, Koutcher D, Ballon B, et al. Iododeoxyuridine (IUDR) uptake and retention as a measure of tumor growth. J Nucl Med 1993;34:1152–61.

[13] Tjuvajev JG, Macapinlac HA, Daghighian F, Scott AM, Ginos JZ, Finn RD, et al. Imaging of the brain tumor proliferative activity with [^{131}I]iododeoxyuridine. J Nucl Med 1994;35:1407–17.

[14] Wakanabe KA, Reichman U, Hirota K, Lopez C, Fox JJ. Nucleosides 110. Synthesis and antiherpes virus activity of some 2′-fluoro-2′-deoxyarabinofuranosylpyrimidine nucleosides. J Med Chem 1979;22:21–4.

[15] Alauddin MM, Conti PS, Fissekis JD. Synthesis of [^{18}F]-labeled 2′-deoxy-2′-fluoro-5-methyl-1-β-D-arabinofuranosyluracil ([^{18}F]-FMAU). J Label Compd Radiopharm 2002;45:583–90.

[16] Conti PS, Alauddin MM, Fissekis JR, Schmall B, Watanabe KA. Synthesis of 2′-fluoro-5-[^{11}C]-methyl-1-β-D-arabinofuranosyluracil

([^{11}C]-FMAU): a potential nucleoside analog for in vivo study of cellular proliferation with PET. Nucl Med Biol 1995;22:783–9.

[17] Mangner TJ, Klecker RW, Anderson L, Shields AF. Synthesis of 2′ -deoxy-2′ -[^{18}F]fluoro-β-D-arabinofuranosyl nucleosides, [^{18}F]FAU, [^{18}F]FMAU, [^{18}F]FBAU and [^{18}F]FIAU, as potential PET agents for imaging cellular proliferation. Synthesis of [^{18}F]labelled FAU. FMAU, FBAU, FIAU. Nucl Med Biol 2003;30:215–24.

[18] Sun H, Solan A, Mangner TJ, Vaishampayan U, Muzik O, Collins JM, et al. Imaging DNA synthesis with [^{18}F]FMAU and positron emission tomography in patients with cancer. Eur J Nucl Med Mol Imaging 2005;32:15–22.

[19] Grant AJ, Feinberg A, Chou TC, Watanabe KA, Fox JJ, Philips FS. Incorporation of metabolites of 2′ -fluoro-5-iodo-1-β-D-arabinofuranosylcytosine into deoxyribonucleic acid of neoplastic and normal mammalian tissues. Biochem Pharmacol 1982;31:1103–8.

[20] Shields AF, Grierson JR, Dohmen BM, Machulla HJ, Stayanoff JC, Lawhorn-Crews JM, et al. Imaging proliferation in vivo with [F-18]FLT and positron emission tomography. Nat Med 1998;4:1334–6.

[21] Cheng YC, Dutschman G, Fox JJ, Watanabe KA, Machida H. Differential activity of potential antiviral nucleoside analogs on herpes simplex virus-induced and human cellular thymidine kinases. Antimicrob Agents Chemother 1981;20:420–3.

[22] Wang J, Eriksson S. Phosphorylation of the anti-hepatitis B nucleoside analog 1-(2′ -deoxy-2′ -fluoro-1-β-D-arabinofuranosyl)-5-iodouracil (FIAU) by human cytosolic and mitochondrial thymidine kinase and implications for cytotoxicity. Antimicrob Agents Chemother 1996;40: 1555–7.

[23] Toyohara J, Waki A, Takamatsu S, Yonekura Y, Magata Y, Fujibayashi Y. Basis of FLT as a cell proliferation marker: comparative uptake studies with [^{3}H]thymidine and [^{3}H]arabinothymidine, and cell-analysis in 22 asynchronously growing tumor cell lines. Nucl Med Biol 2002;29:281–7.

[24] Grierson JR, Shields AF. Radiosynthesis of 3′ -deoxy-3′ -[^{18}F]fluorothymidine: [^{18}F]FLT for imaging of cellular proliferation in vivo. Nucl Med Biol 2000;27:143–56.

[25] Grierson JR, Schwartz JL, Muzi M, Jordan R, Krohn KA. Metabolism of 3′ -deoxy-3′ -[F-18]fluorothymidine in proliferating A549 cells: validations for positron emission tomography. Nucl Med Biol 2004;31:829–37.

[26] Ditmann H, Dohman BM, Kehlbach R, Bartusek G, Pritzkow M, Sarbia M, et al. Early changes in [^{18}F]FLT uptake after chemotherapy: an experimental study. Eur J Nucl Med Mol Imaging 2002;29:1462–9.

[27] Rahim SG, Trivedi N, Bogunovic-Batchelor MV, Hardy GW, Mills G, Selway JW, et al. Synthesis and anti-herpes virus activity of 2′ -deoxy-4′ -thiopyrimidine nucleosides. J Med Chem 1996;39:789–95.

[28] Toyohara J, Hayashi A, Sato M, Tanaka H, Haraguchi K, Yoshimura Y, et al. Rationale of 5-^{125}I-4′ -thio-2′ -deoxyuridine as a potential iodinated proliferation marker. J Nucl Med 2002;43:1218–26.

[29] Toyohara J, Gogami A, Hayashi A, Yonekura Y, Fujibayashi Y. Pharmacokinetics and metabolism of 5-^{125}I-4′ -thio-2′ -deoxyuridine in rodents. J Nucl Med 2003;44:1671–6.

[30] Griengl H, Wanek E, Schwarz W, Steicher W, Rosenwirth B, Clercq ED. 2′ -Fluorinated arabinonucleosides of 5-(2-haloalkyl)uracil: synthesis and antiviral activity. J Med Chem 1987;30:1199–204.

[31] Walker R, Coe P, Rahim SG. Further antiviral pyrimidine nucleosides. International Publication WO9104982.

[32] Ogilvie KK, Beaucage SL, Gillen MF, Entwistle D, Quilliam M. Fluoride ion catalyzed alkylation of purines, pyrimidines, nucleosides and nucleotides using alkyl halides. Nucleic Acid Res 1979;6: 1695–708.

[33] Balzarini J, Celen S, Karlsson A, de Groot T, Verbruggen A, Bormans G. The effect of a methyl or 2-fluoroethyl substituent at the N-3 position of thymidine, 3′ -fluoro-3′ -deoxythymidine and 1-β-D-arabinosylthymine on their antiviral and cytostatic activity in cell culture. Antivir Chem Chemother 2006;17:17–23.

[34] Otter GP, Elzagheid MI, Johens GD, MacCulloch AC, Walker RT, Oivanen M, et al. Synthesis and hydrolytic stability of the α and β anomers of 4′ -thio-2′ -deoxyuridine and their 5-substituted analogs. Competition between the acid-catalysed depyrimidination and isomerisation to 5-thiopyranoside nucleoside. J Chem Soc Perkin Trans 1998;2:2343–9.

[35] Lunato AJ, Wang J, Woollard JE, Anisuzzaman AKM, Ji W, Rong FG, et al. Synthesis of 5-(carboranylalkylmercapto)-2′ -deoxyuridines and 3-(carboranylalkyl)thymidines and their evaluation as substrates for human thymidine kinases 1 and 2. J Med Chem 1999;42:3378–89.

[36] Chi DY, Kilbour MR, Katzenellenbogen JA, Brodack JW, Welch MJ. Synthesis of no-carrier-added *N*-([^{18}F]fluoroalkyl)spiperone derivatives. Appl Radiat Isot 1986;37:1173–80.

[37] Sasaki T, Minamoto K, Suzuki H. Elimination reaction on the di- and trimesylated derivatives of N^3-benzyluridine. J Org Chem 1973;38: 598–607.

[38] Yamamoto I, Kimura T, Tateoka Y, Watanabe K, Ho IK. *N*-substituted oxopyrimidines and nucleosides: structure–activity relationship for hypnotic activity as central nervous system depressant. J Med Chem 1987;30:2227–31.

[39] Fissekis JD, Myles A, Brown GB. Synthesis of 5-hydroxyalkylpyrimidines from lactones. J Org Chem 1964;29:2670–3.

[40] Dyson MR, Coe PL, Walker RT. An improved synthesis of benzyl 3,5-di-*O*-benzyl-2-deoxy-1,4-dithio-D-*erythro*-pentofuranoside, an intermediate in the synthesis of 4′ -thionucleosides. Carbohydr Res 1991;216:237–48.

[41] Edgell WF, Parts L. Synthesis of alkyl and substituted alkyl fluorides from *p*-toluenesulfonic acid esters. The preparation of *p*-toluenesulfonic acid esters of lower alcohols. J Am Chem Soc 1955;77:4899–902.

[42] Wilds CJ, Damha MJ. 2′ -Deoxy-2′ -fluoro-β-D-arabinonucleosides and oligonucleotides (2′ F-ANA): synthesis and physicochemical studies. Nucleic Acids Res 2000;28:3625–35.

[43] Bradshaw Jr MD, Deininger PL. Human thymidine kinase gene: molecular cloning and nucleotide sequence of a cDNA expressible in mammalian cells. Mol Cell Biol 1984;11:2316–20.

[44] Gati P, Misra HK, Knaus EE, Wiebe LI. Structural modifications at the 2′ - and 3′ -positions of some pyrimidine nucleosides as determinations of their interaction with the mouse erythrocyte nucleoside transporter. Biochem Pharmacol 1984;33:3325–31.

[45] Gati WP, Knaus EE, Wiebe LI. Interaction of 2′ -halogeno-2′ -deoxyuridines with the human erythrocyte nucleoside transport mechanism. Mol Pharmacol 1983;23:146–52.

[46] Komatsu T, Yamazaki H, Shimada N, Nagayama S, Kawaguchi Y, Nakajima M, et al. Involvement of microsomal cytochrome p450 and cytosolic thymidine phosphorylase in 5-fluorouracil formation from tegaful in human liver. Cancer Res 2001;7:675–81.

[47] Al-Madhoun AS, Johnsamuel J, Barth RF, Tjarks W, Eriksson S. Evaluation of human thymidine kinase 1 substrates as new candidates for boron neutron capture therapy. Cancer Res 2004;64: 6280–6.

[48] Byun Y, Yan J, Al-Madhoun AS, Johnsamuel J, Yang W, Barth RF, et al. Synthesis and biological evaluation of neutral and zwitterionic 3-carboranyl thymidine analogues for boron neutron capture therapy. J Med Chem 2005;48:1188–98.

[49] Hanes CS. Studies of plant amylases: I. The effect of starch concentration upon the velocity of hydrolysis by the amylase of germinated barley. Biochem J 1932;26:1406–21.

[50] Dixon M. The determination of enzyme inhibitor constants. Biochem J 1953;55:170–1.

[51] Dixon M, Webb EC. Inhibitors. In: Dixon EC, Webb DC, editors. Enzymes. 3rd ed. London: Longman; 1979. p. 332–80.

[52] Eisenthal R, Cornish-Bowden A. The direct linear plot. A new graphical procedure for estimating enzyme kinetic parameters. Biochem J 1974;139:715–20.

[53] Johansson NG, Eriksson S. Structure–activity relationships for phosphorylation of nucleoside analogs to monophosphates by nucleoside kinases. Acta Biochim Pol 1996;43:143–60.

[54] Eriksson S, Kierdaszuk B, Munch-Petersen B, Öberg B, Johansson NG. Comparison of the substrate specificities of human thymidine kinase 1 and 2 and deoxycytidine kinase toward antiviral and cytostatic nucleoside analogs. Biochem Biophys Res Commun 1991;176:586–92.

[55] Al-Madhoun AS, Tjarks W, Eriksson S. The role of thymidine kinases in the activation of pyrimidine nucleoside analogs. Mini Rev Med Chem 2004;4:341–50.

[56] Al-Madhoun AS, Johansamuel J, Yan J, Ji W, Wang J, Zhou JC, et al. Synthesis of a small library of 3-(carboranylalkyl)thymidines and their biological evaluation as substrates for human thymidine kinase 1 and 2. J Med Chem 2002;45:4018–28.

[57] Tjarks W, Wang J, Chandra S, Ji W, Zhuo J, Lunato AJ, et al. Synthesis and biological evaluation of boronated nucleosides for boron neutron capture therapy (BNCT) of cancer. Nucleosides Nucleotides Nucleic Acids 2001;20:695–8.

[58] Kong W, Engel K, Wang J. Mammalian nucleoside transporters. Curr Drug Metab 2004;5:63–84.

[59] Paterson ARP, Cass CE. Transport of nucleoside drugs in animal cells. In: Goldman ID, editor. Membrane transport of antineoplastic agents. New York: Pergamon Press; 1986. p. 309–29.

[60] Plagemann PGW, Wohlhueter RM. Permeation of nucleosides, nucleic acid bases, and nucleotides in animal cells. Curr Top Membr Transp 1980;14:225–330.

[61] Jarvi SM. Adenosine transporters. In: Cooper DMF, Londons C, editors. Adenosine receptors. New York: Alan R. Liss, Inc.; 1988. p. 113–23.

[62] Belt JA. Heterogeneity of nucleoside transport in mammalian cells. Two types of transport activity in L1210 and other cultured neoplastic cells. Mol Pharmacol 1983;24:479–84.

[63] Plagemann PGW, Wohlhueter RM. Nucleoside transport in cultured mammalian cells. Multiple forms with different sensitivity to inhibition by nitrobenzylthioinosine or hypoxantine. Biochem Biophys Acta 1984;773:39–52.

[64] Belt JA, Noel LD. Nucleoside transport in walker 256 rat carcinosarcoma and S49 mouse lymphoma cells. Biochem J 1985; 232:681–8.

[65] Jarvis SM, Young JD. Nucleoside transport in rat erythrocytes: two components with differences in sensitivity to inhibition by nitrobenzylthioinosine and *p*-chloromercuryphenyl sulfonate. J Membr Biol 1986;93:1–10.

[66] Griffith DA, Jarvis SM. Nucleoside and nucleobase transport systems of mammalian cells. Biochem Biophys Acta 1996;1286:153–81.

[67] Belt JA, Marina NM, Phelps DA, Crawford CR. Nucleoside transport in normal and neoplastic cells. Adv Enzyme Regul 1993;33:235–52.

[68] Kornberg A, Baker TA. Biosynthesis of DNA precursors. In: Kornberg A, Baker TA, editors. DNA replication. 2nd ed. New York: Freeman; 1992. p. 53–100.

資料(10)

資料 10

Available online at www.sciencedirect.com

ScienceDirect

Nuclear Medicine and Biology 33 (2006) 765–772

NUCLEAR MEDICINE — AND — BIOLOGY

www.elsevier.com/locate/nucmedbio

Alkyl-fluorinated thymidine derivatives for imaging cell proliferation II. Synthesis and evaluation of N^3-(2-[^{18}F]fluoroethyl)-thymidine

Jun Toyohara[a,*], Akio Hayashi[b], Akie Gogami[b], Yasuhisa Fujibayashi[c]

[a]*Probe Research Section, Department of Molecular Probe, Molecular Imaging Center, National Institute of Radiological Sciences, Chiba 263-8555, Japan*

[b]*Research and Development Division, Research Center, Nihon Medi-Physics Co., Ltd., Chiba, Japan*

[c]*Biomedical Imaging Research Center, University of Fukui, Fukui, Japan*

Received 17 January 2006; revised 16 May 2006; accepted 11 June 2006

Abstract

We prepared N^3-(2-[^{18}F]fluoroethyl)-thymidine ([^{18}F]NFT202) and examined its potential as a positron emission tomography (PET) ligand for imaging cellular proliferation. [^{18}F]NFT202 was synthesized from 3′,5′-di-*O*-toluoyl-N^3-(2-*p*-toluenesulfoxyethyl)-thymidine in a two-step reaction. N^3-(2-fluoroethyl)-[2-^{14}C]thymidine ([^{14}C]NFT202) was also synthesized from [2-^{14}C]thymidine in a one-step reaction. Whereas [^{18}F]NFT202 did not accumulate in mouse Lewis lung carcinoma tumors, 3′-[^{18}F]3′-fluoro-3′-deoxythymidine ([^{18}F]FLT) showed significantly high uptake. To clarify this unexpected result, we evaluated the cell uptake of [^{14}C]NFT202 in vitro. The uptake was approximately eight times higher in thymidine kinase 1 (TK1)$^+$ clones (L-M cells) than in TK1-deficient mutant L-M(TK$^-$) cells ($P<.01$, Student's t test). In addition, we observed a positive correlation between tracer uptake and the S-phase fraction. However, the net in vitro tumor cell uptake of [^{14}C]NFT202 was lower than that of [2-^{14}C]3′-fluoro-3′-deoxythymidine. [^{14}C]NFT202 was not effectively incorporated into the DNA fraction and was indeed washed out from tumor cells. These results clearly showed that [^{18}F]NFT202 did not surpass the performance of [^{18}F]FLT. We therefore conclude that [^{18}F]NFT202 is not a suitable PET ligand for imaging tumor cell proliferation.

Keywords: Nucleosides; Positron emission tomography; Proliferation; [^{18}F]NFT202

1. Introduction

During the last four decades, deoxynucleoside analogs have grown increasingly important in the treatment of viral diseases and cancers. Nucleoside analogs are prodrugs requiring 5′-phosphorylation to form active nucleotides that can function as inhibitors of viral or cellular replication processes. Therefore, when labeled with a suitable radionuclide, some of these compounds have potential use as radiopharmaceuticals for the noninvasive diagnosis of tumor cell proliferation. To be effective in that role, these compounds should have at least the following attributes: (a) they should be selectively phosphorylated by thymidine kinase 1 (TK1); (b) they should be labeled with a positron-emitting or a single-photon-emitting radionuclide; (c) they should exhibit good in vivo stability; and (d) their transport across cell membranes should be rapid.

In a separate paper, our group identified the N^3 fluoroethylated derivative of thymidine, N^3-(2-fluoroethyl)-thymidine (subsequently referred to as NFT202), as a potential agent of cellular proliferation imaging by virtue of three basic properties: (a) it is resistant to glycosidic bond cleavage; (b) its phosphorylation by TK1 is comparable to that by thymidine; and (c) it has an affinity for mammalian 6-[(4-nitroxyl)thiol]-9-β-D-ribofuranosylpurine-sensitive nucleoside transporters. Therefore, we expected fluorine-18-labeled NFT202 to be a suitable tracer for cellular proliferation imaging by positron emission tomography (PET).

In this paper, we describe the synthesis of N^3-(2-[^{18}F]fluoroethyl)-thymidine ([^{18}F]NFT202; **6**) and examine its potential as a PET ligand for imaging cellular proliferation. Despite its acceptable properties in vitro, [^{18}F]NFT202 did not accumulate in tumors. To clarify this result and the uptake mechanism of [^{18}F]NFT202, we also performed an in vitro cell uptake study with N^3-(2-fluoroethyl)-[2-^{14}C]thymidine ([^{14}C]NFT202). Based on resultant data, we concluded that [^{18}F]NFT202 is not a suitable PET ligand for imaging tumor cell proliferation.

* Corresponding author. Tel.: +81 43 206 4041; fax: +81 43 206 3261.
E-mail address: toyohara@nirs.go.jp (J. Toyohara).

0969-8051/$ – see front matter © 2006 Elsevier Inc. All rights reserved.
doi:10.1016/j.nucmedbio.2006.06.001

Moreover, in a number of important ways, this paper parallels previous validation studies with FLT, particularly uptake/washout studies in A549 cells [1]. Nucleoside tracer validation is also discussed.

2. Materials and methods

2.1. Radiochemicals

[2-^{14}C]3′-Fluoro-3′-deoxythymidine ([^{14}C]FLT; 1.961 GBq/mmol, 3.7 MBq/ml) was purchased from Moravek Biochemicals, Inc. (Brea, CA, USA). [2-^{14}C]Thymidine ([^{14}C]Thd; 2.18 GBq/mmol, 3.7 MBq/ml) was purchased from Amersham Biosciences (Piscataway, NJ, USA).

2.2. 3′,5′-Di-O-toluoyl thymidine (2)

p-Toluoyl chloride (2.1 ml, 16.1 mmol) was added to a solution of thymidine (**1**) (1.95 g, 8 mmol) in pyridine (80 ml) under argon atmosphere. The mixture was stirred for 16 h at room temperature and then poured into ice water. After being stirred for 5 min, the precipitated product was collected, washed with water and dried. The desired product (**2**; 3.4 g, 7.1 mmol, 89%) was purified by silica gel column chromatography (*n*-hexane:ethyl acetate=3:1):

^{1}H nuclear magnetic resonance (NMR) (CD_3OD, 500 MHz): δ 8.45 (bs, 1H, NH), 7.69 (m, 4H, *o*-Tol), 7.26 (m, 5H, H-6, *m*-Tol), 6.46 (dd, H-1′, $J_{1',\ 2'a}$=4.4 Hz, $J_{1',\ 2'b}$=6.8 Hz), 5.64 (m, 1H, H-3′), 4.79 (dd, 1H, H-5′a, $J_{5'a,\ 4'}$=2.8 Hz, $J_{5'a,\ 5'b}$=9.6 Hz), 4.65 (dd, 1H, H-5′b, $J_{5'b,\ 4}$=2.8 Hz, $J_{5'b,\ 5'a}$=9.6 Hz), 5.53 (m, 1H, H-4′), 2.70 (ddd, 1H, H-2′a, $J_{2'a,\ 3'}$=1.2 Hz, $J_{2'a,\ 1'}$=4.4 Hz, $J_{2'a,\ 2'b}$=11.2 Hz), 2.44, 2.43 (each s, each 3H, Tol-CH_3), 2.31 (ddd, 1H, H-2′b, $J_{2'b,\ 3'}$=5.2 Hz, $J_{2'b,\ 1'}$=6.8 Hz, $J_{2'b,\ 2'a}$=11.2 Hz), 1.62 (s, 3H, 5-CH_3)

^{13}C NMR ($CDCl_3$, 100 MHz): δ 166.10, 166.04, 163.06, 150.11, 144.64, 134.44, 129.85, 129.53, 129.51, 129.32, 126.54, 126.25, 111.64, 84.91, 82.82, 77.28, 74.91, 64.18, 38.08, 21.76, 21.72, 12.13

mp=200°C

Fast atom bombardment mass spectrometry (FAB-MS): *m/z*=479 [M+H]

High-resolution mass spectrometry (HRMS) for $C_{26}H_{27}N_2O_7$: calculated=479.1819, found=479.1755.

2.3. 3′,5′-Di-O-toluoyl-N^3-(2-hydroxyethyl)-thymidine (3)

Tetrabutylammonium fluoride (TBAF; 20.9 g, 80 mmol) in tetrahydrofuran (THF; 80 ml) and 2-bromoethanol (14 ml, 0.2 mmol) was added to a solution of Compound **2** (3.7 g, 8 mmol) in THF (120 ml) under argon atmosphere. The mixture was stirred for 2 h at room temperature and then poured into ice water. After having been stirred for 5 min, the precipitated product was collected, washed with water and dried (**3**; 3.3 g, 6.5 mmol, 81%):

^{1}H NMR (CD_3OD, 500 MHz): δ 7.96 (m, 4H, *o*-Tol), 7.26 (m, 5H, H-6, *m*-Tol), 6.48 (dd, H-1′, $J_{1',\ 2'a}$=4.4 Hz, $J_{1',\ 2'b}$=6.8 Hz), 5.64 (m, 1H, H-3′), 4.79 (dd, 1H, H-5′a, $J_{5'a,\ 4'}$=2.8 Hz, $J_{5'a,\ 5'b}$=9.6 Hz), 4.66 (dd, 1H, H-5′b, $J_{5'b,\ 4}$=2.8 Hz, $J_{5'b,\ 5'a}$=9.6 Hz), 5.53 (m, 1H, H-4′), 4.21 (m, 1H, H-1′), 3.86 (m, 1H, H-2′), 2.72 (ddd, 1H, H-2′a, $J_{2'a,\ 3'}$=1.2 Hz, $J_{2'a,\ 1'}$=4.4 Hz, $J_{2'a,\ 2'b}$=11.2 Hz), 2.53 (m, 1H, 2′-OH), 2.44, 2.43 (each s, each 3H, Tol-CH_3), 2.31 (ddd, 1H, H-2′b, $J_{2b,\ 3'}$=5.2 Hz, $J_{2b,\ 1'}$=6.8 Hz, $J_{2b,\ 2'a}$=11.2 Hz), 1.65 (s, 3H, 5-CH_3)

^{13}C NMR ($CDCl_3$, 100 MHz) δ 166.06, 166.34, 164.12, 151.56, 144.61, 132.93, 129.81, 129.51, 129.48, 129.30, 126.51, 126.25, 110.99, 85.75, 82.85, 77.25, 74.89, 64.13, 61.79, 43.97, 38.19, 21.73, 21.69, 12.84

mp=180°C

FAB-MS: *m/z*=523 [M+H]

HRMS for $C_{28}H_{31}N_2O_8$: calculated=523.2081, found=523.2026.

2.4. 3′,5′-Di-O-toluoyl-N^3-(2-p-toluenesulfoxyethyl)-thymidine (4)

p-Toluenesulfonyl chloride (229 mg, 1.2 mmol) was added to a solution of Compound **3** (552 mg, 1.0 mmol) in pyridine (10 ml) under argon atmosphere. The mixture was stirred for 16 h at 0°C. After dilution with 50 ml of chloroform, the organic layer was washed with 1 N hydrochloric acid (40 ml), water (40 ml), saturated sodium hydrogen carbonate solution (40 ml) and saturated sodium chloride solution (40 ml). It was then dried by anhydrous sodium sulfate and concentrated. The solvent was removed by rotary evaporation, and the desired product (**4**; 550 mg, 0.74 mmol, 74%) was purified by silica gel column chromatography (n-hexane:ethyl acetate=1:1):

^{1}H NMR (CD_3OD, 500 MHz): δ 7.96 (m, 4H, *o*-Tol), 7.69 (m, 2H, *o*-Ts), 7.26 (m, 7H, H-6, *m*-Tol, *m*-Ts), 6.44 (dd, H-1′, $J_{1',\ 2'a}$=4.4 Hz, $J_{1',\ 2'b}$=6.8 Hz), 5.63 (m, 1H, H-3′), 4.81 (dd, 1H, H-5′a, $J_{5'a,\ 4'}$=2.4 Hz, $J_{5'a,\ 5'b}$=10.0 Hz), 4.65 (dd, 1H, H-5′b, $J_{5'b,\ 4}$=2.8 Hz, $J_{5'b,\ 5'a}$=10.0 Hz), 5.54 (m, 1H, H-4′), 4.27 (m, 1H, H-2′), 4.22 (m, 1H, H-1′), 2.71 (ddd, 1H, H-2′a, $J_{2'a,\ 3'}$=1.2 Hz, $J_{2'a,\ 1'}$=4.4 Hz, $J_{2'a,\ 2'b}$=11.2 Hz), 2.53 (m, 1H, H-2′), 2.45, 2.42, 2.40 (each s, each 3H, Ts-CH_3, Tol-CH_3), 2.28 (ddd, 1H, H-2′b, $J_{2'b,\ 3'}$=5.2 Hz, $J_{2'b,\ 1'}$=6.8 Hz, $J_{2'b,\ 2'a}$=11.2 Hz), 1.58 (s, 3H, 5-CH_3)

^{13}C NMR ($CDCl_3$, 100 MHz): δ 166.05, 166.12, 162.81, 150.60, 144.70, 144.57, 144.55, 132.86, 132.77, 129.79, 129.50, 129.46, 129.28, 127.79, 126.48, 126.25, 110.52, 85.72, 82.86, 77.21, 74.89, 66.30, 64.14, 39.73, 38.09, 21.71, 21.66, 21.55, 12.75

FAB-MS: *m/z*=677 [M+H].

2.5. Radiosynthesis of [^{18}F]NFT202 (6)

[^{18}F]Fluoride was produced with an OSCAR3 cyclotron (Oxford Instruments, Oxon, UK) using ^{18}O-enriched water and ^{18}O(p,n)^{18}F reaction. [^{18}F]Fluoride was separated with an anion exchange resin (SepPak QMA; Nihon Waters KK, Tokyo, Japan). Elution with 66 mM aqueous potassium